Economy-wide and international spillovers of the economic impacts of climate change

Preliminary draft. April 1, 2026.

Maksym Chepeliev[a], Dominique van der Mensbrugghe[b], Toon Vandyck[c]

[a]*The Center for Global Trade Analysis, Purdue University, 403 Mitch Daniels Boulevard, West Lafayette, IN 47907, United States*

[b]*The Center for Global Trade Analysis, Purdue University, 403 Mitch Daniels Boulevard, West Lafayette, IN 47907, United States*

[c]*KU Leuven, Department of Economics, Naamsestraat 69, Leuven, 3000, Belgium*

Abstract

Estimates of the economic consequences of climate change diverge widely and are influenced by methodological choices. Here, we explore different approaches to quantifying economic damages by leveraging a structural model of the global economy. We decompose macroeconomic outcomes by region, factor, and sector to reveal differences between top-down aggregate productivity shocks and a bottom-up representation of impact channels. While aggregate economic outcomes are comparable, region-specific results differ substantially between approaches at the tails of the distribution, driven by divergent international trade responses. Allowing for economic adaptation in production and trade flows, our findings indicate that international spillovers raise global welfare losses from climate change by 1-6% relative to the sum of domestic impacts. Overall, our results suggest that a disaggregated representation of climate change impact channels is important for improving the understanding of aggregate economic outcomes and for informing effective adaptation policies that account for international trade spillovers.

Keywords: Climate impacts, International trade, Economic modeling
JEL classification: F18, Q54, Q56

* Corresponding author: Maksym Chepeliev
Email addresses: mchepeli@purdue.edu (Maksym Chepeliev), vandermd@purdue.edu (Dominique van der Mensbrugghe), toon.vandyck@kuleuven.be (Toon Vandyck)

Economy-wide and international spillovers of the economic impacts of climate change

Abstract

Estimates of the economic consequences of climate change diverge widely and are influenced by methodological choices. Here, we explore different approaches to quantifying economic damages by leveraging a structural model of the global economy. We decompose macroeconomic outcomes by region, factor, and sector to reveal differences between top-down aggregate productivity shocks and a bottom-up representation of impact channels. While aggregate economic outcomes are comparable, region-specific results differ substantially between approaches at the tails of the distribution, driven by divergent international trade responses. Allowing for economic adaptation in production and trade flows, our findings indicate that international spillovers raise global welfare losses from climate change by 1-6% relative to the sum of domestic impacts. Overall, our results suggest that a disaggregated representation of climate change impact channels is important for improving the understanding of aggregate economic outcomes and for informing effective adaptation policies that account for international trade spillovers.

1. Introduction

Developing an improved quantitative understanding of the economic impacts of climate change is crucial to inform the design of efficient adaptation and mitigation policy packages. In addition to non-market impacts, such as human health (Carleton et al., 2022), climate change will affect economic outcomes through a variety of channels that jointly risk lowering economic progress unequally across the globe (Burke, Hsiang, and Miguel, 2015a).

While these impacts are potentially large at the aggregate level, there are various nuances and sources of uncertainty in the quantification. These include the distinction between short- and long-run impacts (Tol, 2018) and the role of adaptation (Burke and Emerick, 2016); the quantification of the impacts of extreme events and natural disasters (Botzen, Deschenes, and Sanders, 2019; Hsiang and Jina, 2014); the presence of tipping points (Dietz et al., 2021); the persistence of shocks and whether these induce level or growth effects on GDP (Nath, Ramey, and Klenow, 2024; Casey, Fried, and Goode, 2023); the role of inequality aversion in quantifying welfare implications (Tol, 2010; Anthoff and Emmerling, 2019; Kornek et al., 2021); the extent to which future damages should be discounted (Guo et al., 2006); and the valuation of non-market goods (Sterner and Persson, 2008; Drupp and Hänsel, 2021). This has led some studies to evaluate and decompose some of these uncertainties in a systematic way (Anthoff and Tol, 2013; Moore et al., 2024).

One of the sources of heterogeneity in the estimates of the economic impacts of climate change lies in the methods used. Top-down econometric work (statistical models) aims to identify causal impacts of changing climatic conditions on aggregate economic outcomes directly. Bottom-up structural modelling, on the other hand, integrates empirical evidence by impact channel (see Auffhammer (2018) for a discussion). Top-down empirical estimates (Burke, Hsiang, and Miguel, 2015b) tend to find larger impacts than bottom-up model-based research, although bottom-up work has advanced to partially close that gap (van der Wijst et al., 2023). However, some of the more recent top-down empirical work (Neal, Newell, and Pitman, 2025; Bilal and Känzig, 2024) indicates economic damages that are much larger than previous estimates, reopening questions about the physical impact channels that could explain these results. As these studies use global rather than local temperatures, they highlight the potential role of cross-country spillovers in determining economic impacts of climate change.

In view of these divergences, Morris et al. (2025) highlight the need to better understand the drivers behind the macro-economic impacts of climate change. They identify evaluating and reconciling the differences in methodologies as a research priority and call on the scientific community to strengthen the associated methodological approaches. In this context, several important methodological aspects of quantifying climate impacts remain underexplored.

First, bottom-up studies usually provide estimates of climate change across multiple impact channels, including agricultural yield changes, labor productivity, land availability, livestock heat stress (Roson and Sartori, 2016; van der Wijst et al., 2023). However, the analysis of impacts of changing climate is often conducted either for selected channels (Moore et al., 2017; Sheng et al., 2025; Schinko et al., 2020) or for multiple channels combined without explicit decomposition of impact mechanisms (van der Wijst et al., 2023; World Bank Group, 2023). At the same time, studies with available decomposition analyses are usually conducted within a single-country context (Arndt, Asante, and Thurlow, 2015). Providing such a decomposition would help to better understand the contribution of each climate impacts channel and potential consequences of not including some them in the analysis in terms of both economy-wide and sectoral implications, as well as facilitate the exploratory analysis of interaction channels across various climate impact mechanisms.

Second, most of the analyses conducted so far do not provide sufficient understanding of the spillover effects on climate damages across countries and regions. Earlier research has either focused on the assessment of climate impacts for specific geographies (World Bank Group, 2023; Arndt, Asante, and Thurlow, 2015; Manuel et al., 2021) or impact channels (Sun et al., 2024; Feng, Li, and Wang, 2025), or use aggregate shocks (Schenker and Osberghaus, 2025; Constant and Davin, 2019). While climate change is the global phenomenon, climate damage shocks are transmitted across countries through international trade channels, while individual countries can also implement specific adaptation measures, thus reducing direct climate damages. In this context, it is essential to understand the geographical spillovers of climate impacts across countries, which will allow to better design adaptation measures and support the decision-making process.

Finally, another important aspect of the climate impacts not sufficiently analyzed in the literature includes the understanding of how climate damages derived from the top-down estimates impact various production factors within the economy. Econometric estimates available in the literature, report climate impacts on GDP (Neal, Newell, and Pitman, 2025; Bilal and Känzig, 2024; Casey, Fried, and Goode, 2023), which are then translated to factor productivity impacts in the economy-wide models. However, different models have different sets of production factors and varying interpretation of those impacted by climate change. For instance, under some approaches only capital and/or labor is shocked, while other models might cover also land and natural resources, with some expanding also to intermediate inputs (Casey, Fried, and Gibson, 2024; Morris et al., 2025). Naturally, the difference in the choices of production factors under climate impact might have substantial implications for the magnitude of estimated results. In addition, a question of the contribution of each production factor damage channel and interactions between them is an important aspect in terms of designing robust adaptation measures.

Here, we address the identified gaps in the literature in terms of a more comprehensive understanding of the climate impact transmission channels, geographical spillovers, and production factor coverage of the climate damages. Relying on the comparison of different approaches to using top-down and bottom-up estimates of climate change damages in a structural model of the global economy, our analysis provides three specific contributions to the existing literature. First, we utilize available bottom-up estimates and provide a comprehensive decomposition of climate impacts across multiple damage channels, quantifying interactions and spillovers across the transmission channels. Second, we quantify geographical spillovers of climate impacts utilizing both top-down and bottom-up damage functions. Finally, the study provides a decomposition of climate damages derived from the top-down estimates across various production factors of the economy. Jointly, these contributions are valuable for informing methodological choices in economic assessments of climate change.

Our comparisons focus both on the temporal, global, and inter-regional implications of climate impacts, as well as highlight various impact channels within the decomposition analysis. In addition to a better understanding of climate impact channels, inter-sectoral, and geographical spillovers, our analysis provides an important contribution to supporting climate adaptation efforts by revealing key drivers behind the damages caused by global warming.

The remainder of the paper is organized as follows. Section 2 provides an overview of the methodological approach, including a description of the applied modeling framework and the scenarios. Section 3 discusses the results of our analysis, including a detailed comparison across two approaches, as well as various decomposition analyses. Finally, Section 4 discusses implications of our analysis for the decision-making and modeling communities, and concludes by drawing key insights for future methodological developments.

2. Methods

2.1. Modelling framework

To assess the implications of climate change, we rely on a global recursive-dynamic computable general equilibrium (CGE) model ENVISAGE (van der Mensbrugghe, 2024). It is a multi-sector multi-region model that is particularly suited for the analysis of climate impacts and mitigation policies, by capturing all key interactions between economic agents within domestic and global markets. The model is solved as a sequence of comparative static equilibria, where the production factors are linked across time periods using the accumulation expressions. The model follows a modular setup, where different modules of the framework can be activated depending on the purpose of the simulations van der Mensbrugghe (2024). The model allows for the parametrization of climate impacts across multiple impact channels, including but not limited to labor heat stress, sea level rise, livestock heat stress, crop yields, impacts on tourism, energy demand, and infrastructural damages. In addition, economy-wide climate impacts could be implemented in the model using total factor productivity or production factor-specific shocks.

The main strength of the global CGE models, like ENVISAGE, is a comprehensive representation of inter-dependencies between sectors, agents, and markets within the economy. By capturing both the supply and demand sides, the model represents adjustments in quantities and prices reacting to various shocks, such as policies, climate, etc. For instance, if a climate shock impacting agricultural crop yields is imposed in the model, this leads to increasing crop prices, reducing crops' supply and demand, accompanied by structural shifts in the economy: declining share of production of the crops that are more impacted by climate change and growing shares of agricultural commodities that experience less adverse climate impacts. In addition, a reallocation of crop supply across countries will take place through international trade flows (e.g., growing share of supplies in the global North). In this regard, the ENVISAGE model incorporates market-based adaptation mechanisms to climate change. Additional details on the ENVISAGE model can be found in van der Mensbrugghe (2024).

The ENVISAGE model used in this paper is calibrated to the Global Trade Analysis Project (GTAP) Power 11 Data Base with 2017 reference year, which represents the global economy across 160 countries/regions and 76 sectors (Aguiar et al., 2023; Chepeliev, 2023). For the purposes of the current study, we use an aggregate of the GTAP-Power Data Base, which includes 27 regions, out of which 19 are individual countries from the G20 list and 30 activities. Details of the sectoral and regional aggregations are available in the Appendix.

2.2. The scenario framework

Our scenario framework consists of the baseline scenario, which represents the evolution of the global economy over 2017-2050 time frame without climate impacts, and a set of climate impact scenarios with various decompositions. In what follows, we first describe the calibration of the baseline scenario and selected growth dynamic features of the ENVISAGE model, then move to the overview of the climate impact scenarios implemented for the paper.

2.2.1. Baseline scenario

The baseline scenario follows the middle-of-the road Shared Socioeconomic Pathways (SSP) 2 path developed by the Organization for Economic Cooperation and Development (OECD) and the International Institute for Applied Systems Analysis (IIASA, 2024). The latter provides population and GDP growth trajectories, with employment growth following the pathway for the population cohort aged between 15 and 64. In the default model closure full employment is assumed, reflecting a long-term labor market assumption. Capital growth assumes the standard capital accumulation formulation. Regional savings adjusts so that the return to capital is broadly unchanged over time. Foreign savings play a relatively minor role and are assumed to decline linearly to 0 by 2040.

Labor productivity in services is calibrated to the given SSP GDP pathway. In agriculture and manufacturing, labor productivity is assumed to be 2 percentage points higher. In the model, this calibrates the variable gl_r. The labor productivity factor is then:

$$\lambda^f_{r,l,a,t} = \lambda^f_{r,l,a,t-1}\left[1 + \chi^f_{r,l,a,t} + gl_{r,t}\right] \tag{1}$$

where gl_r is uniform across activities and χ^f is an additive shifter for agriculture and manufacturing. Capital productivity is calibrated in the baseline using the 'balanced' growth assumption, i.e., the capital/labor ratio measured in efficiency units is constant over time. In the model, this calibrates the variable gk_r. The capital productivity factor is then:

$$\lambda^k_{r,a,v,t} = \lambda^k_{r,a,v,t-1}\left[1 + \chi^k_{r,a,v,t} + gk_{r,t}\right] \tag{2}$$

where gk_r is uniform across activities and χ^f is an additive shifter, which is set to 0 in the baseline.[1] The baseline scenario in the developed assessment framework is calibrated over 2017-2050 time horizon. In terms of radiative forcing, the implemented baseline scenario corresponds to the RCP45 projections.

2.2.2. Climate impact scenarios

The paper considers two sets of climate impact shocks, representing top-down and bottom-up estimates of climate impacts. In the case of top-down estimates, climate impact shocks are sourced from Casey, Fried, and Goode (2023). The shocks are presented as changes to total factor productivity (TFP), which are provided for each year, and are assumed to be uniform across sectors. Let the shock be represented by δ^c_r. This is implemented as a shock to the 'TFP' factor, which is at the top of the production nest and impacts demand for the non-energy intermediate demand bundle and the value added plus energy bundle.

$$TFP_{r,a,t} = TFP^{BaU}_{r,a,t}\left[1 + \delta^c_{r,t}\right] \tag{3}$$

In other words, the EPA shock is applied to the baseline value of TFP (which is equal to 1 for all time periods, sectors, and regions).

In addition, we develop the decomposition of the sources of growth in the following manner:

$$Y = Y(F_f, \lambda_f)$$
$$\frac{\Delta Y}{Y} = \sum_f s_f \frac{\Delta F_f}{F_f} + \sum_f s_f \frac{\Delta \lambda_f}{\lambda_f}$$

where f represents a set of production factors, including capital, labor, land and intermediate inputs. While our default assumption includes that all production factors are impacted by climate change, the decomposition analysis allows to disentangle the contribution of each individual production factor to the aggregate outcome of the climate shock.

For the bottom-up estimates of climate impacts we rely on the shocks developed in Roson and Sartori (2016) complemented with selected additional data sources and refinements, as further discussed in the Appendix. The shocks are implemented across six impact channels. The latter include the following: sea level rise and related changes in agricultural land availability, impacts on crop yields and agricultural productivity, heat stress implications for labor productivity, heat effect on human health, and the impact of climate change on tourism revenues. The model specification allows us to implement these climate impacts across sector and factor-specific channels (where relevant), thus capturing the structural heterogeneity of the climate impacts. As in the case of the top-down shocks decomposition, we also perform a

[1] The index v represents vintage. In the current framework, we only have one vintage.

decomposition of the bottom-up estimates of climate impacts by separating the contribution across five channels discussed above. A detailed discussion on the parametrization and implementation of the bottom-up climate shocks is available in the Appendix.

3. Results

3.1. Bottom-up vs top-down approaches to quantifying climate damages

As discussed earlier, the economic impacts of climate change vary substantially between studies and approaches (Morris et al., 2025; Tol, 2018). Since in the current study we rely on two representative estimates from the top-down and bottom-up approaches respectively, each with its unique underlying assumptions, representing two individual draws from a wide range of available estimates, it is important to explore how these two approaches compare against each other and within the broader set of estimates reported in the literature. Therefore, in this subsection, we focus on comparing global impacts across the two utilized sources of climate impact damages, facilitating such a comparison with decomposition analysis of the production factors coverage for the case of top-down approach.

At the global level, results suggest that the magnitudes of climate impacts on aggregate GDP by 2050 are very similar across both climate impacts parametrization sources (Figure 1a). By 2050, both studies suggest that the global GDP declines by around 0.4-0.6% relative to the baseline with no climate impacts. Temporal dynamics suggests that the bottom-up estimates (based on Roson and Sartori (2016), also referred to as R&S) imply more substantial adverse impacts of climate change at the beginning of the period compared to the top-down shocks from Casey, Fried, and Goode (2023) (referred to as CFG). However, by the end of the period, impacts of the CFG shocks become somewhat larger than the R&S impacts, and based on the continuation of this beyond 2050, the divergence might further increase over time, potentially leading to larger differences across assessment approaches (however, the post-2050 time frame is beyond the scope of our analysis).

When compared to earlier studies, the magnitude of estimated impacts of the R&S approach is comparable to the results reported in other structural studies (Tol, 2018; Morris et al., 2025). Estimated top-down impacts are, however, lower than those reported in most previous econometric studies, as the latter often find damages exceeding 5-10% even for the 2°C warming Morris et al. (2025). Such a difference is driven by the fact that the top-down damages used in the current study are sourced from Casey, Fried, and Goode (2023), who assume in their estimation a transitional (temporary) rather than a steady-state (permanent) impact of temperature changes. While in the latter case the magnitude of impacts is substantially larger, the authors find more empirical evidence to support the transitional (temporary) nature of climate impacts and thus use it for the default estimation approach, resulting in a lower magnitude of the overall climate damages, as compared to some of the earlier top-down estimates.

Decomposition of the CFG climate impacts across production factors implies that the shock to intermediate inputs corresponds to the largest contribution across all considered factors, followed by capital and labor (Figure 1a). As the share of land input in the total mix of economy-wide production factors is relatively small in most countries, the contribution of this production factor to the overall climate damages under the adopted top-down shocks is relatively small (less than 10% of the aggregate damages at the global level).

To further examine the role of including intermediate inputs into the set of production factors when implementing top-down climate impacts, we provide an across-country decomposition of the effects of climate change (Figure 1b). The latter compares country-specific impacts of the TFP shock with (blue) and without (pink) inclusion of the intermediate inputs into the set of production factors facing the climate shock. While in both cases the distribution of impacts across countries is similar, inclusion of the intermediate inputs on average makes the distribution of impacts across countries more pronounced (i.e. steeper second-order polynomial curve), increasing both losses and gains across countries, from the levels observed prior to the coverage of intermediate inputs (Figure 1b).

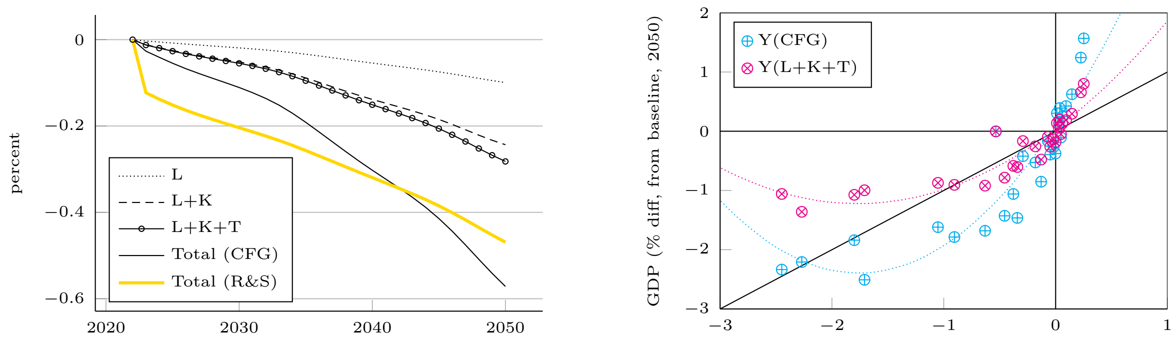

(a) Global impact over time

(b) 2050 impact across countries

Figure 1: Impacts of climate change on GDP. CFG, based on Casey, Fried, and Goode (2023); R&S, based on Roson and Sartori (2016). Top-down shocks (CFG) shocks are applied to labor (L), capital (K), land (T), and output (all factors plus intermediate inputs). All shocks are based on SSP2-RCP45 projections. Panel b includes second-order polynomials to describe the relation between results of different approaches.

3.2. Decomposing economic impacts of climate change

In terms of distribution of impacts across countries, both approaches identify a similar set of winners and losers from climate change. Countries and regions in the global South, including India, Indonesia, South and East Asia, as well as Sub-Saharan Africa, are among those that are impacted the most adversely due to climate damages, with India losing up to 2.5% of GDP in 2050 under both top-down and bottom-up shocks (Figure 2a). On the other hand, high- and upper-middle income countries in the global North, including Russia, Canada, the United Kingdom, South Korea, and a number of European Union countries are among those that experience moderate gains due to climate change under both climate shock implementations (Figure 2a). There are, however, differences in country-specific impacts across the two approaches. In the case of the positively-impacted countries, R&S estimates suggest that the benefits are rather limited, in general not exceeding 0.3-0.4% of GDP in 2050 (e.g., in Russia, Canada, Germany) and are primarily associated with increased revenue from tourism flows. At the same time, CFG shocks imply 2-3 times higher benefits for the same set of countries (1–1.5% gains in both Russia and Canada), potentially indicating a presence of broader economy-wide benefits of moderately increasing temperatures for these countries (Figure 2a).

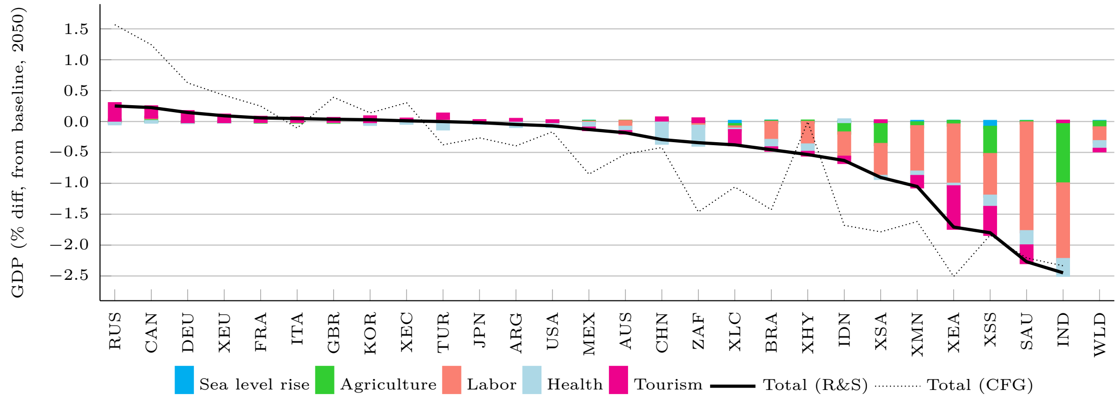

(a) Gross domestic product

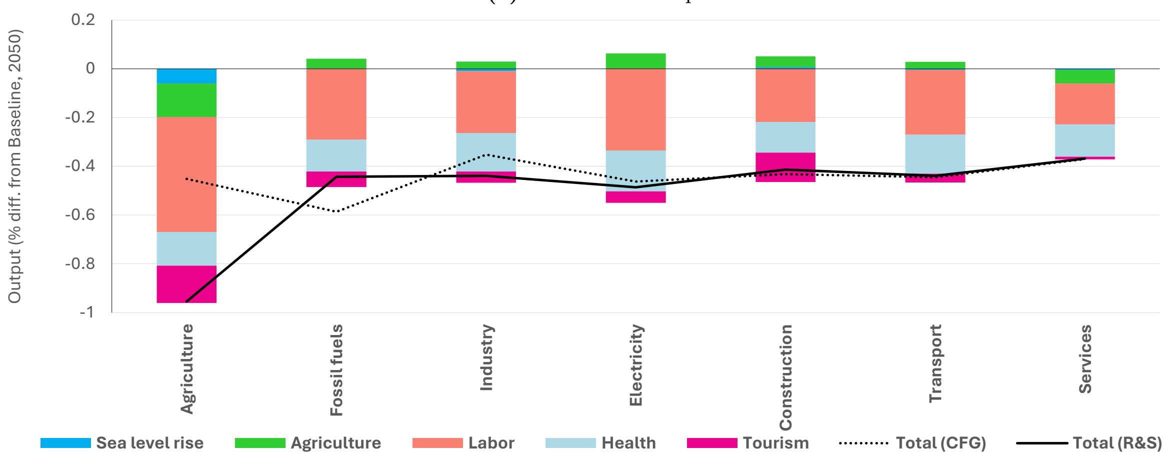

(b) Sectoral output

Figure 2: Decomposition of effects by impact channel. CFG, based on Casey, Fried, and Goode (2023); R&S, based on Roson and Sartori (2016). All shocks are based on SSP2-RCP45 projections.

Overall, top-down shocks tend to imply a higher variability of climate impacts across countries, compared to the bottom-up approach, which applies to both tails of the impact distribution. In the case of most-adversely impacted countries, bottom-up shocks indicate that only 5 out of 27 considered regions experience GDP losses over 1% in 2050. At the same time top-down approach doubles the number of countries (i.e. 10 out of 27), which lose over 1% of their GDP due to climate impacts in 2050 (Figure 2a).

Looking at the decomposition of the bottom-up shocks across impact channels, results suggest that labor impacts represent a substantial contribution in the case of countries that are impacted the most adversely (Figure 2a). However, in the case of three out of four most negatively impacted regions, other impact channels compound the shocks, contributing at least 40% of the total impact (agriculture in the case of Indonesia, tourism in the Rest of East Asia, and both agriculture and tourism in Rest of Sub-Saharan Africa). This implies that in the majority of the most adversely impacted countries, climate damages are caused via multiple major channels, substantially complicating future climate adaptation challenge.

One particular difference between top-down and bottom-up approaches is the representation of the economy-wide spillovers of climate impacts. As top-down shocks assume that impacts occur proportionally across all sectors of the economy, the inter-sectoral variation of impacts at the global level is very moderate, as all activities decline by around 0.4-0.6% in terms of their output in 2050 (Figure 2b). GFC estimates also suggest that fossil fuels are the most adversely impacted economic activity, while industry is the least affected. Top-down estimates, on the other hand, while capturing climate impacts using more refined impact channels and sector-specific damages, suggest a much higher inter-sectoral variation of damages, with agriculture seeing a decline in output of almost 1% and services being the least impacted (output reduction under 0.4%) (Figure 2b).

Further decomposition of the top-down shocks across impact channels highlights several spillover effects (Figure 2b). First, sector-specific shocks, such as agricultural productivity, tend to allocate losses to the directly-impacted sector, while often benefiting other sectors, as production resources (e.g. capital, labor) are allocated away from the impacted sector toward other sectors. Second, sector-specific shocks with substantial implications for purchasing power could have major inter-sectoral spillovers. For instance, this is the case of tourism shock, which, despite impacting a specific activity, results in lower economy-wide revenue through upstream (e.g. transportation and agri-food industry) and downstream (e.g. other services) linkages. Finally, such a decomposition stresses the importance of accounting for multiple channels of climate change impacts - both direct and indirect - as for any given sector, there is no single channel that accounts for over 75% of the total damages, while in some sectors (e.g. agriculture and services) the corresponding contribution is below 50% (Figure 2b).

3.3. International spillovers

As countries are connected via trade flows, economic impacts from climate change in one part of the world can affect economic outcomes in other regions. We now zoom in on these international spillovers, which were implicitly captured in the results presented above.

The existing literature points to a double role of international trade in the context of climate impacts. On the one hand side, trade can amplify the impacts of climate change by causing disruptions to international supply chains (Sun et al., 2024). More generally, climate change can raise the costs of certain goods, which are transmitted along the value chain as these goods serve as inputs into other sectors. On the other hand, international trade is a channel of adaptation that can relieve some of the economic costs by shifting consumption towards goods from regions with lower vulnerability to climate change (Janssens et al., 2020; Baldos and Hertel, 2015). Sectors in these regions may experience a gain in competitiveness compared to their counterparts in strongly affected areas, and as a result may raise exports and market share.

Building further on the comparison of country-specific impacts between bottom-up and top-down estimates, we now decompose GDP changes across three key components: consumption, investment, and trade. With a few exceptions, consumption and investment impacts are well-aligned between the two implementations, while key differences in results are driven by trade impacts (Fig. 3). Overall, the top-down approach suggests rather moderate impacts of climate shocks on trade in the case of all countries. To a large extent, this is driven by the economy-wide nature of the shock, which does not provide comparative advantages (or disadvantages) to any specific sectors. At the same time, the bottom-up approach has more substantial impact on trade at the sectoral level (including through the tourism channel). When the two approaches (bottom-up and top-down) are compared across GDP components, the results also reveal that it is primarily the trade channel that contributes to the reduction of the magnitude of climate impacts on both tails of the impact distribution (Fig. 3).

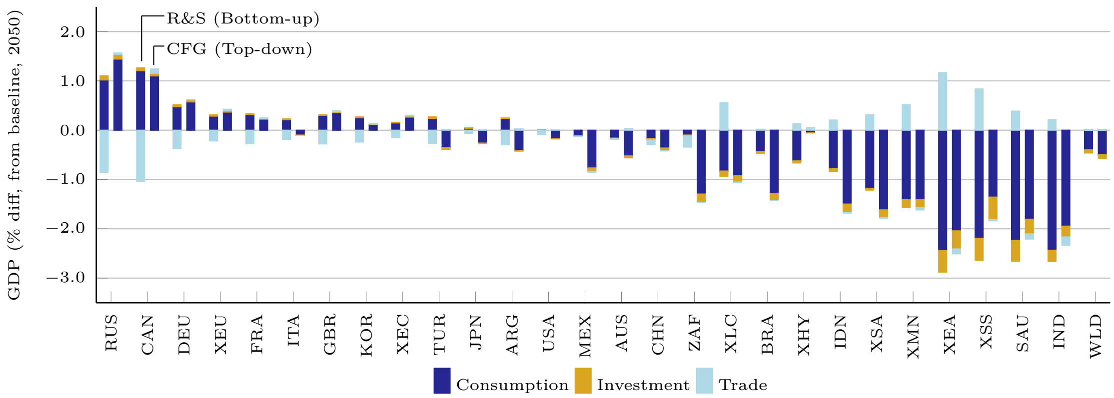

Figure 3: Decomposition of GDP impacts. CFG, based on Casey, Fried, and Goode (2023); R&S, based on Roson and Sartori (2016). All shocks are based on SSP2-RCP45 projections.

To assess international spillovers in more detail, we implement key scenarios [2] on a region-by-region basis, where we introduce climate impacts for one region at a time. Comparing the sum of domestic impacts in these scenarios with outcomes of a global scenario—where all regions face climate impacts simultaneously—yields an estimate of the amplification effect via international trade. Numerical results indicate that this international spillover effect raises global economic damages around 1–6% (see Table C.16) relative to the domestic-only impacts. These estimates account for economic adaptation, as trade flows and production choices endogenously adjust to changing relative prices.

Despite similar aggregate magnitudes, the underlying pattern of international spillovers differs markedly between top-down and bottom-up implementations. Figure 4 presents bilateral spillovers in terms of welfare impacts (measured as equivalent variation). In the top-down approach (panel a), the sign of the spillovers mostly reflects the direction of the domestic impact: gains from climate change are passed on to trading partners (e.g., from Russia to the Rest of Europe and Central Asia region (XEC)), while damages also cause negative cross-border welfare impacts (e.g., from USA to Canada and Mexico). However, a few notable exceptions emerge. Climate damages in India, for example, benefit welfare in China, and vice versa, indicating changes in comparative advantage on Asian and global markets. The top-down analysis furthermore picks up some indirect effects. For instance, the USA gains from positive climate change impacts in Canada, while Mexico sees a welfare decline as some of the USA's imports are redirected from Mexico to Canada.

The bottom-up representation of climate change impacts results in a more mixed and

[2] We focus here on capital and labor productivity in the top-down approach, as in Casey, Fried, and Goode (2023). For the bottom-up approach, we exclude tourism as the shock is set up for a multi-regional setting to ensure global balance, as described in Appendix A.5.

asymmetric pattern of bilateral welfare spillovers (panel b). Tailoring the implementation of climate shocks to specific sectors increases the heterogeneity of effects, creating more scope for adjustments of relative competitiveness and corresponding trade flows. For instance, the Rest of East Asia and Pacific (XEA) gains from climate impacts in India by raising exports of agricultural products and processed food, illustrating spillovers across both sectors and space. More generally, a pattern emerges where regions that are only moderately affected by climate change (such as Turkey and Argentina) gain in competitiveness compared to other regions with stronger impacts (India, Sub-Saharan Africa). Correspondingly, the extent to which foreign climate impacts affect domestic welfare is typically larger when impact channels are represented in a bottom-up fashion. Domestic climate impacts represent 90–110% of the total impact for 21 regions in the top-down approach, while this is the case for only 9 regions in the bottom-up approach (see Table C.17).

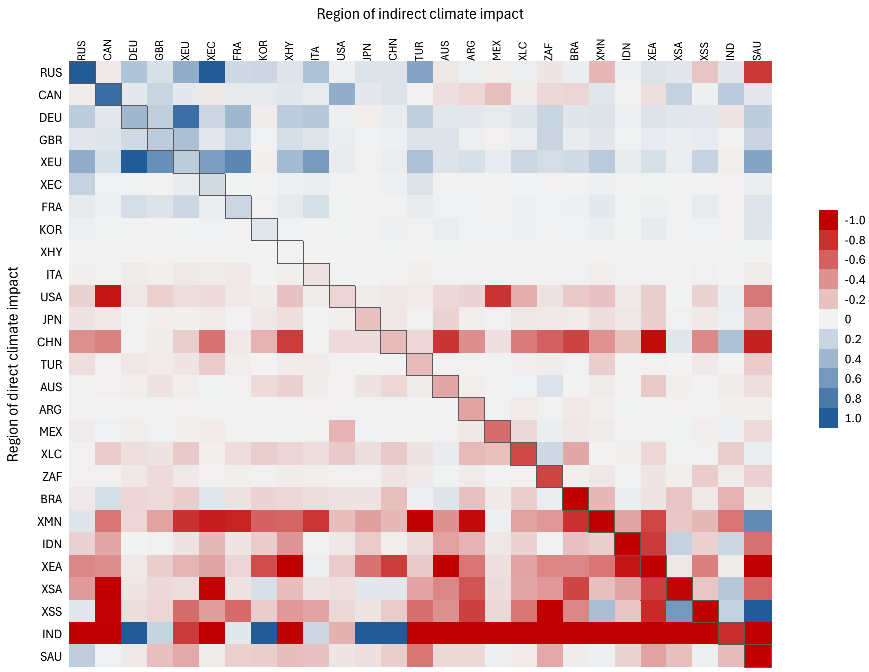

(a) Top-down specification (K+L)

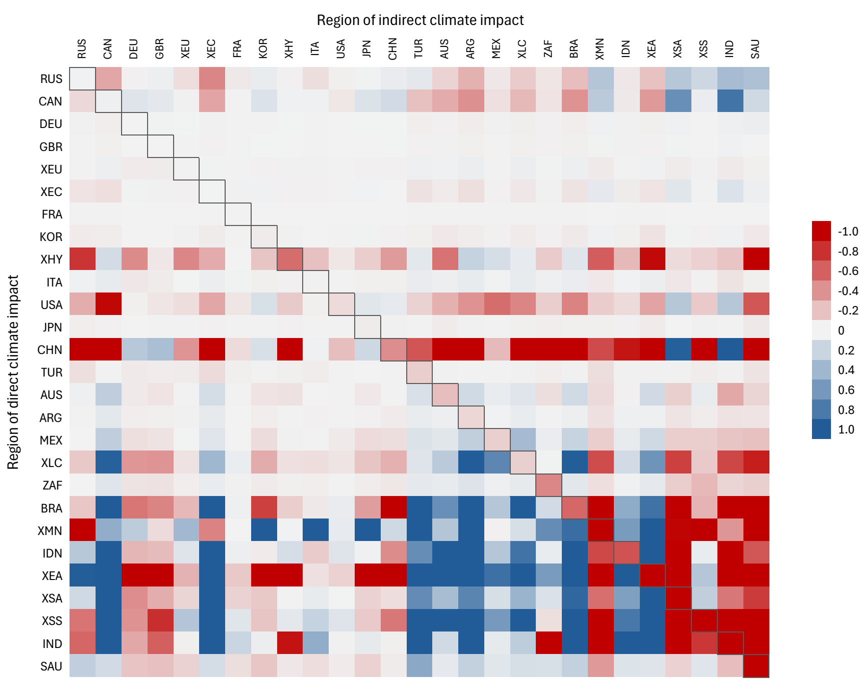

(b) Bottom-up specification (SLR+AGR+LAB+HLT)

Figure 4: International spillovers from climate impacts. Rows indicate the region where the climate shock is implemented. The diagonal shows the corresponding welfare impacts (%). Off-diagonal elements represent indirect welfare impacts (10^{-2} %) in other countries (in the columns).

4. Discussion and conclusion

Structural economic models are pivotal in quantifying the macroeconomic impacts of climate change. The work presented in this paper aims at improving our understanding of methodological aspects related to economy-wide modeling of climate change impacts. Our findings suggest that even when aggregate impacts of selected bottom-up and top-down approaches align relatively well, divergent trade impacts between different modeling approaches illustrate the value added of using damage curves by impact channels based on biophysical models in an economy-wide model with sectoral detail. Future work may test the robustness of these findings when expanding the inputs for the shocks to a broader empirical base that includes more channels and recent evidence.

Our analysis reveals several important methodological findings to inform future research. First, when considering the choice of the production factors impacted by the climate damages, our findings suggest that intermediate inputs are by far the most substantial factor in terms of driving overall impacts, contributing even more substantially than capital, labor and land combined. Inclusion of intermediate inputs into the overall set of shocked factors also makes the distribution of both gains and losses of climate impacts more pronounced, implying both the change in magnitudes and the slope of the inter-country incidence effects. This highlights the importance of the decision regarding the factor coverage in the model when implementing TFP-derived climate shocks. To our knowledge, the empirical literature on the impacts of climate change on intermediate inputs is thin. Further research could inform future model-based assessments on this aspect.

Second, we find strong sectoral spillover effects across climate impact channels, highlighting the importance of accounting for both direct and indirect climate damages across multiple channels, even when focusing the assessment on a specific sector. For instance, in the case of agriculture, yield shocks—often analyzed as the single agricultural climate impact channel in earlier studies (Baldos and Hertel, 2014; Wheeler and Von Braun, 2013)—account for less than 15% of the total impact. Recent papers highlight the need of accounting for labor productivity shocks in agriculture in addition to yield impacts (e.g. de Lima et al. (2021))—however, our findings suggest that even these two channels combined explain less than two thirds of the overall damages in the agricultural sector. Similar strong interaction effects are also found in other sectors, as there is no single climate impact channel that accounts for more than three quarters of the overall impact in any single sector, even when both direct and indirect (spillovers from other sectors) impacts are taken into account for each channel.

Third, the numerical results presented in this paper illustrate that international spillovers can play a significant role in the quantification of the economic impacts of climate change, as impacts are transmitted along value chains and across borders. Comparing aggregate productivity shocks with detailed modeling by impact channel, we show how aggregate approaches risk overlooking important trade responses to climate change.

The research presented in this paper furthermore yields policy-relevant insights. Importantly, our findings suggest that adaptation policy would benefit from acknowledging interaction effects that put regions' economic resilience at risk through compounding impacts. A proper design of adaptation policies should recognize the contribution of each climate impact channel, as well as the distribution of direct and indirect impacts. For instance, while yield impacts have been widely acknowledged as a major channel through which climate change affects agriculture, our results suggest that it is ranked fourth in terms of the overall damages for this sector. Therefore, focusing the majority of adaptation efforts on this single channel might not be the most efficient policy option. In this regard, quantifying the ranking of climate impacts and identifying the amplification channels can offer valuable insights for designing cost-effective adaptation policies. In addition, this paper highlights the relevance of international collaboration on climate change adaptation, as simple economic reasoning—that governments make socially optimal adaptation decisions as both the corresponding costs and benefits are borne locally—breaks down when international spillovers are strong (Feng, Li, and Wang, 2025).

Our analysis can be extended in various directions. One particularly promising research area includes a better understanding of market-mediated adaptations to climate impacts and the role of trade both as a buffer and a transmitter of climate shocks. Economy-wide modeling frameworks, like the one used in the current study, endogenously include a number of adjustment mechanisms. Buffering mechanisms include the reallocation of production factors from more to less impacted sectors, changes in the allocation of production between domestic and foreign markets, as well as adjustments in the geographical composition of trade, among others. By incorporating these adjustment mechanisms, economy-wide models already include market-driven adaptations, which are not always presented in other approaches or might not be well-revealed in historical data due to a relatively low magnitude of the observed climate shocks. In this regard, it is important to better understand the role of these market-mediated adjustments, and their observed magnitudes in both the short and the long run. These aspects could be explored more in-depth by comprehensively adjusting model parametrization, changing substitution and transformation possibilities across different agents and inputs, activating and deactivating selected adjustment channels, building on empirical evidence.

Our assessment includes a parametrization of a range of climate impact channels with the bottom-up estimates. This set of impact channels is incomplete and could be further extended. The limited coverage of impact channels could also explain some of the differences between the implemented bottom-up and top-down estimates. In this regard, inclusion of other climate impact channels, such as livestock heat stress, extreme weather events, energy supply and demand impacts, infrastructural damages, or losses of ecosystem services, could potentially bridge the gap with top-down estimates. In addition, such an expansion would also help to enrich the decomposition analysis implemented here, providing additional policy insights.

In addition, a more comprehensive decomposition analysis using a wider range of both bottom-up and top-down assessments of climate impacts will be of particular importance, considering a broad range of available estimates (see Howard and Sterner (2025) for a recent review). Conducting a more systematic comparison and decomposition analysis would allow for a better understanding of differences between the two assessment approaches while enhancing the robustness of the findings highlighted in this study.

References

Aguiar, A., M. Chepeliev, E. Corong, and D. van der Mensbrugghe. 2023. "The Global Trade Analysis Project (GTAP) Data Base: Version 11." *Journal of Global Economic Analysis*, 7(2). doi:10.21642/JGEA.070201AF.

Anthoff, D., and J. Emmerling. 2019. "Inequality and the social cost of carbon." *Journal of the Association of Environmental and Resource Economists*, 6(2): 243–273.

Anthoff, D., and R.S. Tol. 2013. "The uncertainty about the social cost of carbon: A decomposition analysis using fund." *Climatic change*, 117: 515–530.

Arndt, C., F. Asante, and J. Thurlow. 2015. "Implications of climate change for Ghanaâs economy." *Sustainability*, 7(6): 7214–7231.

Auffhammer, M. 2018. "Quantifying economic damages from climate change." *Journal of Economic Perspectives*, 32(4): 33–52.

Baldos, U.L.C., and T.W. Hertel. 2014. "Global food security in 2050: the role of agricultural productivity and climate change." *Australian Journal of Agricultural and Resource Economics*, 58(4): 554–570.

Baldos, U.L.C., and T.W. Hertel. 2015. "The role of international trade in managing food security risks from climate change." *Food Security*, 7(2): 275–290.

Bilal, A., and D.R. Känzig. 2024. "The macroeconomic impact of climate change: Global vs. local temperature." National Bureau of Economic Research, Report.

Bosello, F., R. Roson, and R.S. Tol. 2006. "Economy-wide estimates of the implications of climate change: Human health." *Ecological Economics*, 58(3): 579–591. doi:10.1016/j.ecolecon.2005.07.032.

Botzen, W.W., O. Deschenes, and M. Sanders. 2019. "The economic impacts of natural disasters: A review of models and empirical studies." *Review of Environmental Economics and Policy*, pp. 167–188.

Burke, M., and K. Emerick. 2016. "Adaptation to climate change: Evidence from US agriculture." *American Economic Journal: Economic Policy*, 8(3): 106–140.

Burke, M., S.M. Hsiang, and E. Miguel. 2015a. "Global non-linear effect of temperature on economic production." *Nature*, 527(7577): 235–239.

Burke, M., S.M. Hsiang, and E. Miguel. 2015b. "Global non-linear effect of temperature on economic production." *Nature*, 527: 235–239. doi:10.1038/nature15725.

Carleton, T., A. Jina, M. Delgado, M. Greenstone, T. Houser, S. Hsiang, A. Hultgren, R.E. Kopp, K.E. McCusker, I. Nath, et al. 2022. "Valuing the global mortality consequences of climate change accounting for adaptation costs and benefits." *The Quarterly Journal of Economics*, 137(4): 2037–2105.

Casey, G., S. Fried, and M. Gibson. 2024. "Understanding climate damages: Consumption versus investment." *European Economic Review*, 167: 104799. doi:https://doi.org/10.1016/j.euroecorev.2024.104799. https://www.sciencedirect.com/science/article/pii/S0014292124001284.

Casey, G., S. Fried, and E. Goode. 2023. "Projecting the Impact of Rising Temperatures: The Role of Macroeconomic Dynamics." *IMF Economic Review*, 71(3): 688–718. doi:10.1057/s41308-023-00203-0.

Chepeliev, M. 2023. "GTAP-Power Data Base: Version 11." *Journal of Global Economic Analysis*, 8(2). doi:10.21642/JGEA.080203AF. https://jgea.org/ojs/index.php/jgea/article/view/222.

Cline, W.R. 2007. *Global Warming and Agriculture: Impact Estimates by Country*. Washington, DC: Center for Global Development and Peterson Institute for International Economics. http://bookstore.piie.com/book-store/4037.html.

Constant, K., and M. Davin. 2019. "Unequal vulnerability to climate change and the transmission of adverse effects through international trade." *Environmental and Resource Economics*, 74(2): 727–759.

de Lima, C.Z., J.R. Buzan, F.C. Moore, U.L. Baldos, M. Huber, and T.W. Hertel. 2021. "Heat stress on agricultural workers exacerbates crop impacts of climate change." *Environmental Research Letters*, 16(4): 044020. doi:10.1088/1748-9326/abeb9f.

Dietz, S., J. Rising, T. Stoerk, and G. Wagner. 2021. "Economic impacts of tipping points in the climate system." *Proceedings of the National Academy of Sciences*, 118(34): e2103081118.

Drupp, M.A., and M.C. Hänsel. 2021. "Relative prices and climate policy: How the scarcity of nonmarket goods drives policy evaluation." *American Economic Journal: Economic Policy*, 13(1): 168–201.

Feng, A., H. Li, and Y. Wang. 2025. "We are All in the Same Boat: Cross-Border Spillovers of Climate Shocks through International Trade and Supply Chains." *The Economic Journal*, 135(669): 1433–1466.

Guo, J., C.J. Hepburn, R.S. Tol, and D. Anthoff. 2006. "Discounting and the social cost of carbon: a closer look at uncertainty." *environmental science & policy*, 9(3): 205–216.

Howard, P.H., and T. Sterner. 2025. "Methodology Matters: A Careful Meta-Analysis of Climate Damages." *Environmental and Resource Economics*, pp. 1–39.

Hsiang, S.M., and A.S. Jina. 2014. "The causal effect of environmental catastrophe on long-run economic growth: Evidence from 6,700 cyclones." National Bureau of Economic Research, Report.

Janssens, C., P. Havlík, T. Krisztin, J. Baker, S. Frank, T. Hasegawa, D. Leclère, S. Ohrel, S. Ragnauth, E. Schmid, et al. 2020. "Global hunger and climate change adaptation through international trade." *Nature climate change*, 10(9): 829–835.

Kornek, U., D. Klenert, O. Edenhofer, and M. Fleurbaey. 2021. "The social cost of carbon and inequality: When local redistribution shapes global carbon prices." *Journal of Environmental Economics and Management*, 107: 102450.

Manuel, L., O. Chiziane, G. Mandhlate, F. Hartley, and E. Tostão. 2021. "Impact of climate change on the agriculture sector and household welfare in Mozambique: an analysis based on a dynamic computable general equilibrium model." *Climatic Change*, 167(1): 6.

Mendelsohn, R., and M.E. Schlesinger. 1999. "Climate-response functions." *Ambio*, 28(4): 362–366. https://www.researchgate.net/publication/285027177_Climate-response_functions.

Moore, F.C., U. Baldos, T. Hertel, and D. Diaz. 2017. "New science of climate change impacts on agriculture implies higher social cost of carbon." *Nature Communications*, 8(1): 1607. doi:10.1038/s41467-017-01792-x.

Moore, F.C., M.A. Drupp, J. Rising, S. Dietz, I. Rudik, and G. Wagner. 2024. "Synthesis of evidence yields high social cost of carbon due to structural model variation and uncertainties." *Proceedings of the National Academy of Sciences*, 121(52): e2410733121.

Morris, J., S.K. Rose, J. Reilly, A. Gurgel, S. Paltsev, and C.A. Schlosser. 2025. "Reconciling widely varying estimates of the global economic impacts from climate change." *Nature Climate Change*, pp. 1–4.

Nath, I.B., V.A. Ramey, and P.J. Klenow. 2024. "How much will global warming cool global growth?" National Bureau of Economic Research, Report.

Neal, T., B.R. Newell, and A. Pitman. 2025. "Reconsidering the macroeconomic damage of severe warming." *Environmental Research Letters*, 20(4): 044029.

Roson, R., and M. Sartori. 2010. "The environmental impact and sustainability applied general equilibrium (ENVISAGE) model. Introducing climate change impacts and adaptation. Changes in the model structure and parameters' estimation." The World Bank, Washington, DC, Mimeo.

Roson, R., and M. Sartori. 2016. "Estimation of Climate Change Damage Functions for 140 Regions in the GTAP 9 Data Base." *Journal of Global Economic Analysis*, 1(2): 78–115. doi:10.21642/JGEA.010202AF.

Schenker, O., and D. Osberghaus. 2025. "International Trade and the Transmission of Temperature Shocks." *Environmental and Resource Economics*, 88(4): 965–1007.

Schinko, T., L. Drouet, Z. Vrontisi, A. Hof, J. Hinkel, J. Mochizuki, V. Bosetti, K. Fragkiadakis, D. Van Vuuren, and D. Lincke. 2020. "Economy-wide effects of coastal flooding due to sea level rise: a multi-model simultaneous treatment of mitigation, adaptation, and residual impacts." *Environmental Research Communications*, 2(1): 015002.

Sheng, D., X. Zhao, J.A. Edmonds, S.T. Morris, P. Patel, B.C. OâNeill, C. Tebaldi, and M.A. Wise. 2025. "Omitting labor responses underestimates the effects of future heat stress on agriculture." *Communications Earth & Environment*, 6: 400. doi:10.1038/s43247-025-02318-w. https://doi.org/10.1038/s43247-025-02318-w.

Sterner, T., and U.M. Persson. 2008. "An even sterner review: Introducing relative prices into the discounting debate." *Review of environmental economics and policy*, pp. 61–76.

Sun, Y., S. Zhu, D. Wang, J. Duan, H. Lu, H. Yin, C. Tan, L. Zhang, M. Zhao, W. Cai, et al. 2024. "Global supply chains amplify economic costs of future extreme heat risk." *Nature*, 627(8005): 797–804.

Tol, R.S. 2018. "The economic impacts of climate change." *Review of environmental economics and policy*, pp. 4–25.

Tol, R.S. 2010. "International inequity aversion and the social cost of carbon." *Climate Change Economics*, 1(01): 21–32.

van der Mensbrugghe, D. 2024. "The Environmental Impact and Sustainability Applied General Equilibrium (ENVISAGE) Model. Version 10.4." Center for Global Trade Analysis (GTAP), Department of Agricultural Economics, Purdue University, West Lafayette, IN, Unpublished manuscript. https://mygeohub.org/groups/gtap/envisage-docs.

van der Wijst, K.I., F. Bosello, S. Dasgupta, L. Drouet, J. Emmerling, A. Hof, M. Leimbach, R. Parrado, F. Piontek, G. Standardi, and D. van Vuuren. 2023. "New damage curves and multimodel analysis suggest lower optimal temperature." *Nature Climate Change*, pp. . doi:10.1038/s41558-023-01636-1.

Wheeler, T., and J. Von Braun. 2013. "Climate change impacts on global food security." *Science*, 341(6145): 508–513.

World Bank Group. 2023. "Azerbaijan Country Climate and Development Report." doi:10.1596/40622. http://hdl.handle.net/10986/40622, License: CC BY-NC-ND 3.0 IGO.

Appendix A. Implementation of Roson and Sartori 2016

This Appendix describes the implementation of the bottom-up estimates of the economic impacts of climate change using the impacts from Roson and Sartori (2016). Roson and Sartori (2016) highlights these bottom-estimates for a number of specific channels including:

- Sea-level rise and its impacts on land available for agriculture
- Crop yields
- Heat stress on labor productivity
- Heat effect on human health
- Tourism revenues

The provided estimates are available as a look-up table for each of the 140 regions in the original V9 GTAP Data Base and for five discrete temperature changes ranging from 1 to 5°C. We went back to the original sources to be able to provide estimates for any set of countries, i.e., not limited to the GTAP regions, and for a continuum of temperature changes, i.e., not limited to interpolating from the Roson & Sartori estimates.

The pathway for the temperature anomalies for each country was provided by the EPA for various SSP/RCP combinations. The impact scenario for this study is the *SSP245* combination. The box and whisker plot in Figure A.5 provides a depiction of the median temperature anomaly and its dispersion across countries.

Appendix A.1. Sea-level rise

The impacts of sea-level rise depend on changes in temperature and the year, due to lagged effects. For each region r, the impact of temperature on the percent change in the amount of land for agriculture is provided by the following equation:

$$\Delta Land_{r,t} = \beta_r^{lnd}\left[\alpha^{SLR} + \beta^{SLR}\Delta T - \gamma_r^{VLM}\right](t - 2000) \tag{A.1}$$

The primary data is based on 5 country-based indicators:

- The percent change in coastal wetland for each SLR of 0.16m. The aggregation is based on the simple average across all countries.
- The percent of erodible coast ($ERDC\_p$). For most countries this is set at 70%. For the European countries the data comes from the EUROSION project. The aggregation is based on the simple average across all countries.
- The percent of relevant coast ($RELC\_p$). The data is sourced from UNEP at a highly aggregated regional level and each country is mapped to a UNEP region. The aggregation is based on the simple average across all countries.
- The sea coast area (measured in km2) ($SEAC\_km$). The aggregation is based on summing the relevant areas.

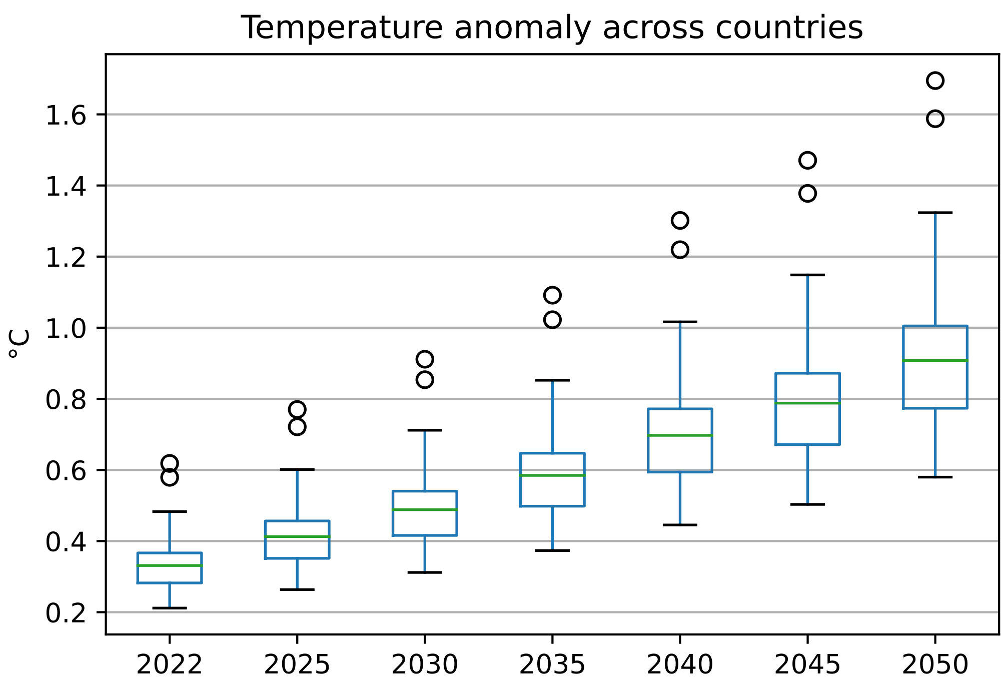

Figure A.5: Projected temperature anomalies across countries used in the bottom-up impact projections.

- Agricultural land (measured in km2) ($AGLND\_km$). The aggregation is based on summing the relevant areas.
- The parameter γ^{VLM}, i.e., estimates of vertical land movement (VLM), are sourced from `sonel.org`. The aggregation is based on the simple average across all countries with a non-zero value for VLM.

The parameter β^{lnd} is calculated from the following formula:

$$\beta_r^{lnd} = \Delta Wetland_r \left(\chi^{erdc} ERDC\_p_r\right) SEAC\_km_r \left(\frac{\chi^{relc} RELC\_p_r}{AGLND\_km_r}\right) \frac{1}{0.16} \tag{A.2}$$

The user can choose the scale parameters, χ^{erdc} and χ^{relc}, which by default are set to 1. In summary, the aggregation facility needs to aggregate the five indicators listed above using the relevant aggregation formula, calculate the parameter β^{lnd} and send the resulting values for β^{lnd} and γ^{VLM} to the output file.

Table A.1 provides the resulting estimates used for this study by modeled region and year.[3] The impact for 2050 is rather limited. The bottom row shows the unweighted average for all modeled regions, which represents the shock to the agricultural land supply curve. The core of the table shows how the average shock is distributed across modeled regions. The

[3] The temperature change per year is for the specific SSP245 Scenario, which was used uniformly used across all studies for this special issue.

hardest hit country in relative terms is Japan, with relatively large shocks for Korea, Rest of East Asia (XEA), rest of Latin America and Caribbean (XLC) and Rest of High-income (XHY). If the shock is applied to the total land area, it would take some 2,660 km^2 out of production—the last column of the table.

Table A.1: The projected impact of sea-level rise on land supply

	2022	2025	2030	2035	2040	2045	2050	Area
AUS	20	19	18	17	16	16	15	-45.5
CHN	2	2	3	3	4	4	4	-16.3
JPN	1171	1176	1180	1183	1186	1231	1227	-175.4
KOR	234	241	246	250	254	265	267	-10.2
IDN	0	0	0	0	0	4	16	-11.7
IND	4	4	4	4	4	4	4	-4.7
CAN	13	57	89	119	145	168	185	-637.3
USA	21	19	18	17	16	17	16	-57.0
MEX	28	26	25	23	22	22	22	-16.4
ARG	3	4	4	5	5	5	6	-6.0
BRA	4	4	4	4	4	4	4	-12.4
FRA	12	11	11	10	10	10	10	-2.1
DEU	7	7	8	8	8	8	8	-1.1
ITA	42	41	40	40	39	41	40	-4.6
GBR	36	35	35	34	34	34	34	-3.2
RUS	50	49	49	48	47	49	48	-308.7
SAU	4	4	4	4	4	4	4	-3.2
TUR	47	46	46	45	45	46	46	-13.9
ZAF	8	8	8	8	8	8	8	-3.7
XEA	290	267	252	236	225	226	217	-404.7
XSA	6	6	6	6	5	6	5	-3.8
XEC	2	2	2	2	2	2	2	-3.7
XMN	54	53	52	51	51	52	51	-187.4
XSS	6	5	5	5	5	5	4	-40.0
XLC	227	215	206	197	189	191	185	-516.4
XEU	40	39	38	37	36	37	36	-39.8
XHY	269	259	251	244	237	242	236	-130.9
Mean:	-7.98e-06	-1.06e-05	-1.45e-05	-1.95e-05	-2.58e-05	-3.11e-05	-3.92e-05	-2660.2

Note: The numbers represent the impact by region relative to the (unweighted) average impact provided on the last row. The final column represents the projected change in land measured in km^2.
Source: Authors.

Appendix A.2. Agriculture

Appendix A.2.1. Crop yields

Impacts on crop yields have been estimated for three crops: rice, wheat and maize. The main equation is:

$$\Delta\, Yield_{r,i}(\Delta T) = \chi^{yld}_{i,trop}(\Delta T) + \left(\chi^{yld}_{i,temp}(\Delta T) - \chi^{yld}_{i,trop}(\Delta T)\right) \frac{Lat_r}{40} \tag{A.3}$$

Table A.2: Original yield impacts

	Temperate					*Tropical*				
	+1°C	+2°C	+3°C	+4°C	+5°C	+1°C	+2°C	+3°C	+4°C	+5°C
Maize	-1%	-3%	-4%	-7%	-11%	-4%	-8%	-10%	-12%	-14%
Wheat	-5%	-6%	-7%	-8%	-9%	4%	-4%	-20%	-34%	-44%
Rice	-4%	-3%	-2%	-7%	-16%	0%	-2%	-4%	-6%	-8%

Source: Roson and Sartori (2016)

Table A.3: Estimated coefficients for yield impacts

	Temperate			*Tropical*		
	Intercept	Linear	Quadratic	Intercept	Linear	Quadratic
Maize		-0.54596	-0.31988		-4.40124	0.32919
Wheat		-3.86957	0.43478		0.59627	-2.01242
Rice	-11.000	8.34286	-1.85714		-0.56522	-0.21739

Source: Authors.

where χ_{trop}^{yld} and χ_{temp}^{yld} are respectively the estimated yields in tropical and temperate zones and *Lat* is the average latitude. Close to the tropics, where the latitude is close to zero, the impact is mostly the tropical impact, and as latitude rises, the yield impact approaches the temperate impact. Roson and Sartori (2016) provide a single table for the impacts across the three crops and two zones for five temperature changes (1-5 C°). There are two solutions for intermediate temperature changes. One is linear interpolation between two provided levels, the other is to approximate a curve for each combination of crop and zone. In either case, the approach is independent of the specific aggregation. The aggregation approach takes the average of the latitude for each of the regional aggregates.[4] The impacts in the paper are provided in Table A.2. The estimated coefficients are provided in Table A.3. In this case, the yield impacts by zone are calculated using:

$$\chi_{i,z}^{yld}(\Delta T) = \chi_{i,z} + \alpha_{i,z}\Delta T + \beta_{i,z}(\Delta T)^2$$

where the estimated coefficients are provided in Table A.2.

Appendix A.2.2. Aggregate agriculture

A second set of impacts has been provided for aggregate agriculture, based on an approach by Mendelsohn and Schlesinger (1999) and as implemented by Cline (2007). The main equation is:

$$\Delta Y = \alpha\Delta T + \beta\left(\Delta T\right)^2 + \gamma\Delta P + \lambda\Delta K/K \tag{A.4}$$

where Y is output per hectare, T is temperature, P is precipitation and K is the atmospheric concentration of CO_2. Roson and Sartori (2016) convert this equation to the following:

[4] This leads to levels quite different from the original GTAP V9 aggregation provided in the paper.

$$\Delta Y = \Delta T \left[\alpha + \gamma p + \lambda k/365 \right] + \beta \left(\Delta T \right)^2 \tag{A.5}$$

where $p = \Delta P/\Delta T$ and $k = \Delta K/\Delta T$, i.e., the change in precipitation and CO_2 relative to the change in temperature and 365 is the original carbon concentration in ppm. The values for the parameters are $\alpha = 115.992$, $\beta = -9.936$, $\gamma = 0.4752$ and $\lambda = 7.884$. Roson and Sartori (2016) provide reference values for temperature and precipitaton, as well as the changes—the latter from an assessment of projections from CMIP5. The value for p is then calculated from $\Delta P/\Delta T$ using the values from CMIP5. The value for k assumes that growth in concentration is a user-provided constant amount for N years, where the values are respectively an increase of 2.11 in CO_2 concentration per year over 70 years, and hence $k = 2.11 \times 70/\Delta T$, where again ΔT is sourced from CMIP5. N.B. In the Excel file, Roson and Sartori (2016) actually calculate the following:

$$\Delta Y = \Delta T \left[\alpha + \gamma p + 10\lambda k/365 \right] + 0.5\beta \left(\Delta T \right)^2 + \beta T \Delta T \tag{A.6}$$

where T is the reference year temperature. They convert this to a percent change in yield by dividing through by an estimate of the initial yield per hectare as measured in dollars.

The Excel file also allows for calculating the regional temperature change if only the average global temperature change is provided.

Table A.4 lists the projected impacts on agricultural productivity used for the bottom-up simulations. The shock is applied to the land factor in all agricultural activities. There are a number of regions that are projected to have positive yield shocks—notably Canada and Russia, and to a lesser extent many regions largely in the temperate zone. Many large regions in the tropical zones will see the reverse, notably Brazil, India, Indonesia and Sub-Saharan Africa.

Appendix A.3. Temperature and labor stress

This section describes the impact of rising temperatures on labor productivity. The original data from Roson and Sartori (2016) is provided as a ’fixed’ table. We describe herein the process of recreating the impact using country level data.

Appendix A.3.1. Data

The first step is to download the data for monthly temperature and precipitation. Roson and Sartori (2016) recommend using data at https://www.weatherbase.com/weather/countryall.php3, but we were unable to access this data. We found an alternative source at https://ourworldindata.org/ (*Our World in Data*). Fortunately, there is an available API that allows for direct access via R or Python. The Python code in the following listing provides simple access to the desired data. The code on lines 9 and 20 allow one to gather any information in the OWID database that has relevance to ’temperature’ and ’precipitation’. This allows us to identify the relevant database that is used to set the appropriate `path` in lines 12 and 24. The downloaded data frames are saved as CSV files.

Listing 1: Accessing *Our World in Data* using Python

```
1 # https://ourworldindata.org/easier-to-reuse-our-data
2 # https://www.allendowney.com/blog/2024/11/24/download-the-world-in-data/
```

Table A.4: The projected impact of temperature rise on agricultural yields

	2022	2025	2030	2035	2040	2045	2050
AUS	-0.00104	-0.00130	-0.00154	-0.00186	-0.00222	-0.00252	-0.00292
CHN	0.00269	0.00332	0.00391	0.00464	0.00549	0.00615	0.00702
JPN	0.00302	0.00345	0.00376	0.00400	0.00406	0.00395	0.00358
KOR	0.00346	0.00396	0.00430	0.00455	0.00461	0.00446	0.00400
IDN	-0.00936	-0.01168	-0.01387	-0.01666	-0.01995	-0.02262	-0.02618
IND	-0.00749	-0.00936	-0.01113	-0.01339	-0.01606	-0.01822	-0.02113
CAN	0.00996	0.01234	0.01454	0.01732	0.02052	0.02306	0.02638
USA	0.00137	0.00169	0.00197	0.00233	0.00274	0.00305	0.00345
MEX	-0.00768	-0.00963	-0.01146	-0.01382	-0.01663	-0.01891	-0.02199
ARG	-0.00207	-0.00263	-0.00317	-0.00389	-0.00477	-0.00550	-0.00651
BRA	-0.00783	-0.00978	-0.01161	-0.01395	-0.01671	-0.01895	-0.02194
FRA	0.00010	0.00012	0.00014	0.00017	0.00019	0.00021	0.00023
DEU	0.00111	0.00137	0.00161	0.00190	0.00224	0.00250	0.00284
ITA	-0.00185	-0.00242	-0.00299	-0.00377	-0.00476	-0.00562	-0.00685
GBR	0.00092	0.00114	0.00134	0.00159	0.00187	0.00209	0.00238
RUS	0.00805	0.00999	0.01178	0.01405	0.01667	0.01876	0.02150
SAU	-0.00715	-0.00894	-0.01062	-0.01277	-0.01532	-0.01738	-0.02015
TUR	0.00349	0.00389	0.00409	0.00413	0.00384	0.00336	0.00238
ZAF	-0.00769	-0.00970	-0.01161	-0.01410	-0.01709	-0.01956	-0.02293
XEA	-0.00794	-0.00993	-0.01178	-0.01417	-0.01697	-0.01924	-0.02228
XSA	-0.00563	-0.00709	-0.00847	-0.01027	-0.01242	-0.01418	-0.01658
XEC	0.00144	0.00176	0.00205	0.00240	0.00279	0.00309	0.00345
XMN	-0.00610	-0.00767	-0.00914	-0.01106	-0.01334	-0.01521	-0.01774
XSS	-0.01018	-0.01273	-0.01512	-0.01819	-0.02181	-0.02475	-0.02869
XLC	-0.00724	-0.00905	-0.01075	-0.01293	-0.01551	-0.01760	-0.02040
XEU	-0.00013	-0.00021	-0.00029	-0.00041	-0.00058	-0.00074	-0.00098
XHY	0.00120	0.00142	0.00160	0.00179	0.00196	0.00205	0.00212

Source: Authors.

```python
import pandas
from owid import catalog

# look for a subject, return a data frame of matches

x = catalog.find('temperature')
if True:

    path = 'garden/climate/2025-01-07/surface_temperature/surface_temperature'

    rc = catalog.RemoteCatalog()
    df = rc[path]

    df.to_csv('v:/Envisage/ClimateDamage/temp.csv', index=True)


x = catalog.find('precipitation')

if True:

    path = 'garden/climate/2025-01-07/total_precipitation/total_precipitation'

    rc = catalog.RemoteCatalog()
    df = rc[path]

    df.to_csv('v:/Envisage/ClimateDamage/prec.csv', index=True)
```

The data requires some additional steps–mainly because the database does not cover all countries that we desire. We map the missing countries to existing countries and/or regions. The mappings are described in Table A.5.

This data is available from 1940-2024. We take the average for the period 1960-2000, for each month and for each country.

Appendix A.3.2. Calculating the wet bulb globe temperature

Roson and Sartori (2016) have estimated the wet bulb globe temperature using data on temperature and precipitation, with an intermediate step, which estimates relative humidity.

$$H_{c,m}(\Delta T) = \chi^H + \alpha^H \left(T_{c,m} + \xi \Delta T\right) + \beta^H P_{c,m} + \beta^{H2} \left(P_{c,m}\right)^2 \qquad (A.7)$$

where T is the average monthly temperature for country c and P is the average monthly precipitation (in mm). In Roson and Sartori (2016), the value of ξ is zero, i.e., they assume no impact on relative humidity from changes in temperature. The values of the coefficients are 67.1082 for the intercept, -0.8438 for temperature, 0.2305 for precipitation, and -0.0005 for precipitation squared.

The estimated WBGT level is given by:

$$WBGT_{c,m}(\Delta T) = \chi^W + \alpha^W \left(T_{c,m} + \Delta T\right) + \beta^W E_{c,m}(\Delta T) \qquad (A.8)$$

$$E_{c,m}(\Delta T) = \chi^E \left(0.01 * H_{c,m}(\Delta T)\right) \exp\left(\frac{\alpha^E (T_{c,m} + \Delta T)}{\beta^E + (T_{c,m} + \Delta T)}\right) \qquad (A.9)$$

where E is the average absolute humidity. The coefficients for the first equation 0.567 for the intercept, 3.94 for temperature and 0.393 for average absolte humidity. The coefficients for the second equation are 6.105 for the shift factor, 17.27 for the numerator of the exponent and 237.7 for the denominator.

Table A.5: Country mapping for climate data

	Country with missing data		Mapping country/region
TWN	Chinese Taipei	HKG	Hong Kong
SGP	Singapore	MYS	Malaysia
MLT	Malta	MED	Mediterranean Region (NIAID)
GUM	Guam	SPC	South Pacific Ocean (NIAID)
MHL	Marshall Islands	SPC	South Pacific Ocean (NIAID)
FSM	Micronesia (Federated States of)	SPC	South Pacific Ocean (NIAID)
NRU	Nauru	SPC	South Pacific Ocean (NIAID)
NFK	Norfolk Island	AUN	Australia (NIAID)
MNP	Northern Mariana Islands	SPC	South Pacific Ocean (NIAID)
NIU	Niue	SPC	South Pacific Ocean (NIAID)
PLW	Palau	SPC	South Pacific Ocean (NIAID)
TKL	Tokelau	SPC	South Pacific Ocean (NIAID)
TON	Tonga	SPC	South Pacific Ocean (NIAID)
TUV	Tuvalu	SPC	South Pacific Ocean (NIAID)
WLF	Wallis and Futuna Islands	SPC	South Pacific Ocean (NIAID)
MAC	Macao	HKG	Hong Kong
BMU	Bermuda	JAM	Jamaica
SPM	Saint Pierre and Miquelon	CAN	Canada
GUF	French Guiana	SUR	Suriname
TCA	Turks and Caicos Islands	JAM	Jamaica
ABW	Aruba	JAM	Jamaica
BRB	Barbados	JAM	Jamaica
DMA	Dominica	JAM	Jamaica
GRD	Grenada	JAM	Jamaica
GLP	Guadeloupe	PRI	Puerto Rico
MTQ	Martinique	PRI	Puerto Rico
MSR	Montserrat	PRI	Puerto Rico
ANT	Netherlands Antilles	PRI	Puerto Rico
KNA	Saint Kitts and Nevis	PRI	Puerto Rico
LCA	Saint Lucia	PRI	Puerto Rico
VGB	British Virgin Islands	PRI	Puerto Rico
LIE	Liechtenstein	CHE	Switzerland
MDA	Republic of Moldova	ROU	Romania
GIB	Gibraltar	ESP	Spain
MCO	Monaco	FRA	France
SMR	San Marino	ITA	Italy
MYT	Mayotte	COM	Comoros
REU	Réunion	COM	Comoros
BVT	Bouvet Island	SAT	South Atlantic Ocean (NIAID)
IOT	British Indian Ocean Territory	SAT	South Atlantic Ocean (NIAID)
ATF	French Southern Territories	SAT	South Atlantic Ocean (NIAID)

Appendix A.3.3. The impact on labor productivity

The impact on productivity is bounded by 100 on the upside, i.e., $WBGT$ is less than a given temperature threshold, and by a minimum level of $\Delta\pi^{min}$ if $WBGT$ goes above a maximum temperature threshold. It declines linearly at the rate ε between the two bounds. Table A.6 provides the default values for the various parameters. Figure A.6 provides a visual depiction of the relation between temperature and its impact on labor productivity.

$$\Delta\pi_{c,i,m}(\Delta T) = \begin{cases} 100 & \text{if } WBGT_{c,m}(\Delta T) < T_i^{min} \\ 100 - \varepsilon_i \left(WBGT_{c,m}(\Delta T) - T_i^{min}\right) & \text{if } T_i^{min} \leq WBGT_{c,m}(\Delta T) < T_i^{max} \\ \Delta\pi_i^{min} & \text{if } WBGT_{c,m}(\Delta T) \geq T_i^{max} \end{cases} \tag{A.10}$$

Table A.6: Parameters for labor stress impact

Sector	$\Delta\pi^{min}$	T^{min}	T^{max}	ε
Agriculture	25	26	36	7.50
Manufacturing	25	28	43	5.00
Services	25	30	50	3.75

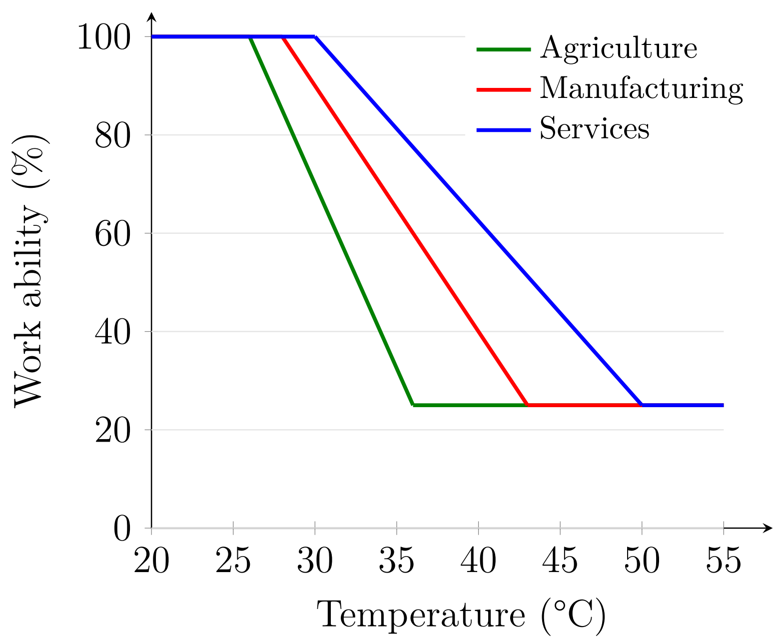

Figure A.6: Work ability (productivity) as a function of WBTG (°C)

In the final step, the monthly labor productivity impact is aggregated across all months and then transformed into a percent decline relative to 1.

$$\Delta\Pi_{c,i}(\Delta T) = 0.01 \left(\frac{1}{12} \sum_m \Delta\pi_{c,i,m}(\Delta T) \right) - 1 \tag{A.11}$$

Table A.7 depicts the shocks to labor productivity that are used for this study. The shocks are differentiated across agriculture, manufacturing and services. Any missing combination implies that there is no projected shock to labor productivity. Not surprisingly, agricultural labor is the most impacted with estimated impacts of 10% and greater in many regions. The shocks are mostly limited to low- and middle-income regions with a few exceptions.

Table A.7: The projected impact of temperature rise on labor productivity

	2022	2025	2030	2035	2040	2045	2050
AUS-AGR	-0.03823	-0.03970	-0.04136	-0.04366	-0.04635	-0.04851	-0.05138
AUS-MAN	-0.00280	-0.00347	-0.00409	-0.00488	-0.00580	-0.00654	-0.00752
JPN-AGR	0.00000	0.00000	0.00000	-0.00024	-0.00100	-0.00162	-0.00244
KOR-AGR	-0.01007	-0.01130	-0.01244	-0.01390	-0.01559	-0.01696	-0.01877
IDN-AGR	-0.05080	-0.05725	-0.06326	-0.07092	-0.07987	-0.08706	-0.09660
IND-AGR	-0.10775	-0.11154	-0.11508	-0.11958	-0.12484	-0.12907	-0.13468
IND-MAN	-0.02441	-0.02618	-0.02783	-0.03022	-0.03326	-0.03571	-0.03910
IND-SRV	-0.00276	-0.00311	-0.00373	-0.00451	-0.00543	-0.00617	-0.00715
MEX-AGR	0.00000	-0.00009	-0.00106	-0.00253	-0.00500	-0.00698	-0.00962
BRA-AGR	-0.05122	-0.05582	-0.06010	-0.06556	-0.07193	-0.07705	-0.08448
BRA-MAN	0.00000	0.00000	0.00000	0.00000	0.00000	0.00000	-0.00045
SAU-AGR	-0.12520	-0.12820	-0.13100	-0.13457	-0.13873	-0.14208	-0.14652
SAU-MAN	-0.04129	-0.04332	-0.04521	-0.04762	-0.05044	-0.05270	-0.05571
SAU-SRV	-0.00817	-0.00909	-0.00996	-0.01106	-0.01234	-0.01337	-0.01474
XEA-AGR	-0.09051	-0.09551	-0.10034	-0.10693	-0.11476	-0.12106	-0.12941
XEA-MAN	-0.00818	-0.00997	-0.01163	-0.01401	-0.01700	-0.01940	-0.02261
XSA-AGR	-0.08238	-0.08643	-0.09023	-0.09515	-0.10110	-0.10590	-0.11225
XSA-MAN	-0.01309	-0.01522	-0.01730	-0.01995	-0.02304	-0.02553	-0.02887
XSA-SRV	0.00000	0.00000	-0.00012	-0.00052	-0.00118	-0.00174	-0.00248
XEC-AGR	-0.00011	-0.00037	-0.00061	-0.00101	-0.00166	-0.00224	-0.00300
XEC-MAN	-0.00000	-0.00000	-0.00000	-0.00000	-0.00005	-0.00015	-0.00028
XMN-AGR	-0.06409	-0.06665	-0.06924	-0.07256	-0.07643	-0.07962	-0.08400
XMN-MAN	-0.01547	-0.01698	-0.01839	-0.02019	-0.02229	-0.02397	-0.02621
XMN-SRV	-0.00268	-0.00328	-0.00383	-0.00454	-0.00542	-0.00621	-0.00727
XSS-AGR	-0.05819	-0.06273	-0.06696	-0.07234	-0.07863	-0.08420	-0.09165
XSS-MAN	-0.00802	-0.00918	-0.01052	-0.01222	-0.01441	-0.01659	-0.01948
XSS-SRV	0.00000	0.00000	-0.00011	-0.00040	-0.00092	-0.00134	-0.00189
XLC-AGR	-0.00086	-0.00173	-0.00338	-0.00548	-0.00810	-0.01092	-0.01559
XHY-AGR	-0.06577	-0.06846	-0.07096	-0.07416	-0.07822	-0.08157	-0.08601
XHY-MAN	-0.01359	-0.01477	-0.01595	-0.01746	-0.01922	-0.02064	-0.02257
XHY-SRV	-0.00050	-0.00068	-0.00085	-0.00110	-0.00159	-0.00199	-0.00251

Source: Authors.

Appendix A.4. Temperature and health stress

Roson and Sartori (2016) provide the impacts on health (measured as a percentage point decline in labor productivity for a 1°C increase in temperature) for the 140 GTAP regions. It is composed of a region-specific shifter and an adjustment factor that is common for all counties mapped to one of the broad regions. The methodology is described below. For our purposes, we simply map health-related productivity impact from the regions in V9 to the countries using the country to region mapping.

Appendix A.4.1. Core data

The original data comes from Table 1 of a paper by Bosello, Roson, and Tol (2006), which describes the additional years of life diseased in 2050, re-produced herein as Table A.8.

Table A.8: Additional years of life diseased in 2050 by region and disease

	Malaria	Schistom.	Dengue	Cardio	Respiratory	Diarrhea	Total
USA	0	0	0	-167,357	22,257	83,070	-62,030
European Union	0	0	0	-171,908	20,936	25,608	-125,364
E & C Europe	0	0	0	-259,884	46,884	57,717	-155,283
Japan	0	0	0	-65,353	33,161	912	-31,280
Rest of Annex I	0	0	0	-45,232	11,108	1,361	-32,763
Energy exporters	7,219	-1,088	29	-66,363	1,706,267	112,633	1,758,697
China & India	632	0	0	-1,119,902	770,340	156,271	-192,659
Rest of the world	232,737	-154,375	203	-194,383	3,683,042	834,294	4,401,518

Source: Bosello, Roson, and Tol (2006).

Roson and Sartori (2016) adjust Table A.8 and convert the *Cardio* and *Respiratory* columns into *Heat* and *Cold* columns. The *Heat* column is equal to some fraction of the *Cardio* column[5] plus all of the *Respiratory* column. The *Cold* column is calculated via residual, i.e., the sum of the *Cardio* and *Respiratory* columns less the *Heat* column. Hence the row sums are identical.

Table A.9: Transformation of Table A.8

	Malaria	Schistom.	Dengue	Heat	Cold	Diarrhea	Total
USA	0	0	0	57,402	-202,502	83,070	-62,030
European Union	0	0	0	43,284	-194,256	25,608	-125,364
E & C Europe	0	0	0	83,086	-296,086	57,717	-155,283
Japan	0	0	0	56,982	-89,174	912	-31,280
Rest of Annex I	0	0	0	27,595	-61,719	1,361	-32,763
Energy exporters	7,219	-1,088	29	1,732,149	-92,245	112,633	1,758,697
China & India	632	0	0	1,193,663	-1,543,225	156,271	-192,659
Rest of the world	232,737	-154,375	203	3,743,923	-255,264	834,294	4,401,518

Source: Roson and Sartori (2016).

Roson and Sartori (2016) make further adjustments:

1. Scale the malaria, schistomiasis, dengue and cold columns—the default scale factors are 1.33, 0, 0.1 and 0, respectively, i.e., the results exclude impacts from schistomiasis and cold.
2. Add a row for *Africa* which is a replication of the *Rest of the world* data.
3. Delete the impacts of malaria and dengue for *Energy exporters* and *Rest of the world*.

The results of these adjustments lead to the final table.

[5] The scale factors in order of the regions in the table are: -0.21, -0.13, -0.1393, -0.3645, -0.3645, -0.39, -0.378 and -0.3132.

Table A.10: Final table of additional years of life diseased in 2050

	Malaria	Schistom.	Dengue	Heat	Cold	Diarrhea	Total
USA	0	0	0	57,402	0	83,070	140,472
European Union	0	0	0	43,284	0	25,608	68,892
E & C Europe	0	0	0	83,086	0	57,717	140,803
Japan	0	0	0	56,982	0	912	57,894
Rest of Annex I	0	0	0	27,595	0	1,361	28,956
Energy exporters	0	0	0	1,732,149	0	112,633	1,844,782
China & India	843	0	0	1,193,663	0	156,271	1,350,777
Rest of the world	0	0	0	3,743,923	0	834,294	4,578,217
Africa	310,316	0	20	3,743,923	0	834,294	4,888,553

Source: Roson and Sartori (2016).

Appendix A.4.2. Updating the health-related productivity impacts

Table A.8 was used as a starting point for estimates of the labor productivity impacts of health in an earlier version of Envisage (Roson and Sartori (2010)) using the GTAP V7 regional definition. These older estimates are the starting point for the estimates. For each country, mapped to one of the broad regions from above, the new estimate is equal to the old estimate plus an additive shifter, which is uniform across all countries in the mapping. The idea behind the shifter is that it should reflect the changes between Table A.9 and Table A.10. In the case of Japan, for example, the original health impact in levels of additional years in 2050 jumps to nearly 58 thousand, compared with a decline of just above 31 thousand in the earlier estimate. The original productivity impact was 3.4%, which drops to -6.3% with the updated table. Roson and Sartori (2016) use a minimization algorithm to calculate the region-specific shifter, which minimizes the distance between the aggregate changes in the tables and the estimated changes. To be more precise, the targeted change from the tables is calculated as:

$$\tau_R^t = Table A.10_{R,Total}/Table A.9_{R,Total} - 1$$

In the case of Africa, the target is an increase of +11%. The original average impact in Africa was a drop in health-related labor productivity of around 0.57%. The adjustment pushes this down to a productivity loss of 0.63%. The mathematical setup is as follows: (1) equation (A.12) is the new estimate of the productivity loss, which is equal to the original estimate plus the uniform shifter (δ_R) for all regions r mapped to broad region R[6]; (2) equation (A.13) creates an $r \times R$ matrix with the updated estimates of the labor productivity impact; (3) equation (A.14) calculates the average deviation in the productivity impact with respect to the original estimate, where M^0 is the relevant matrix with the initial productivity estimates, i.e., with π^0; and (4) equation (A.15) is the objective function, which is a quadratic loss function in terms of the average deviation of the new productivity estimates and the targeted deviation, which is determined at the aggregate regional level. The minimization process is done for each aggregate region separately.

6 The matrix A is a mapping matrix with 1's and 0's.

$$\pi_r^1 = \pi_r^0 + \sum_R A_{r,R}\delta_R \tag{A.12}$$

$$M_{r,R}^1 = \sum_R A_{r,R}\pi_r^1 \tag{A.13}$$

$$\tau_R^v = \frac{\sum_r M_{r,R}^1}{\sum_r M_{r,R}^0} - 1 \tag{A.14}$$

$$Obj = \left(\tau_R^v - \tau_R^t\right)^2 \tag{A.15}$$

Table A.11 provides a summary of the impacts on health-related labor productivity from using the new health impacts as provided in TableA.10 relative to the earlier estimates in A.9. For many regions, the health-related impacts move from positive to negative and in some cases are numerically significant, for example the countries mapped to the *China & India* region.

Table A.11: Changes in health-related labor productivity for the broad regions

Region	Value
USA	-0.127
European Union	-0.093
E & C Europe	-0.132
Japan	-0.097
Rest of Annex I	-0.112
Energy exporters	-0.020
China & India	-0.614
Rest of the world	-0.006
Africa	-0.059

Source: Roson and Sartori (2016).

Table A.12 re-produces the health-related labor productivity shocks introduced into the bottom-up simulations. The level of the shock is modest relative to the heat-related labor stress shocks described in the previous section. The highest impacts occur in China, India, Saudi Arabia and South Africa, but none reaches even a 1% impact on labor productivity. The two labor shocks are implemented cumulatively using the following expression:

$$\lambda_{r,l,a,t} = \lambda_{r,l,a,t}^{BaU}\left(1 + \chi_{r,s,t}^{heat}\right)\left(1 + \chi_{r,t}^{health}\right)$$

where each activity a is mapped to one of the three broad sectors (s), i.e., agriculture, manufacturing and services, and λ and λ^{BaU} represent respectively labor productivity in the current and baseline scenarios.

Appendix A.5. Impact on tourism revenues

The starting point for the tourism impact is data on tourist arrivals and departures, both in terms of number of persons and the total amount spent. For example, Italy had arrivals of some 51 million persons who spent \$43 billion, or roughly \$850 per person. On the other hand, Italian departures amounted to some 21 million persons, spending \$28.7 billion, or an average of some \$1,363. Arrivals is an exponential function of temperature and temperature

Table A.12: The projected impact of temperature rise on health-related labor productivity

	2022	2025	2030	2035	2040	2045	2050
AUS	-0.00033	-0.00041	-0.00048	-0.00058	-0.00069	-0.00078	-0.00090
CHN	-0.00188	-0.00234	-0.00277	-0.00331	-0.00395	-0.00446	-0.00515
JPN	-0.00014	-0.00017	-0.00020	-0.00025	-0.00029	-0.00033	-0.00038
KOR	-0.00015	-0.00019	-0.00022	-0.00027	-0.00032	-0.00036	-0.00041
IDN	0.00024	0.00030	0.00036	0.00043	0.00051	0.00058	0.00067
IND	-0.00251	-0.00312	-0.00370	-0.00443	-0.00528	-0.00597	-0.00688
USA	-0.00048	-0.00060	-0.00071	-0.00085	-0.00101	-0.00114	-0.00132
MEX	-0.00072	-0.00089	-0.00106	-0.00126	-0.00151	-0.00170	-0.00196
ARG	-0.00049	-0.00061	-0.00073	-0.00087	-0.00104	-0.00117	-0.00135
BRA	-0.00060	-0.00074	-0.00088	-0.00105	-0.00125	-0.00142	-0.00163
FRA	-0.00000	-0.00000	-0.00000	-0.00000	-0.00000	-0.00000	-0.00000
DEU	-0.00000	-0.00000	-0.00000	-0.00000	-0.00000	-0.00000	-0.00000
ITA	-0.00000	-0.00000	-0.00000	-0.00000	-0.00000	-0.00000	-0.00000
GBR	-0.00000	-0.00000	-0.00000	-0.00000	-0.00000	-0.00000	-0.00000
RUS	-0.00010	-0.00012	-0.00015	-0.00018	-0.00021	-0.00024	-0.00027
SAU	-0.00137	-0.00171	-0.00202	-0.00242	-0.00289	-0.00326	-0.00376
TUR	-0.00106	-0.00132	-0.00156	-0.00187	-0.00223	-0.00252	-0.00290
ZAF	-0.00147	-0.00184	-0.00217	-0.00260	-0.00310	-0.00350	-0.00404
XEA	-0.00012	-0.00015	-0.00018	-0.00021	-0.00026	-0.00029	-0.00033
XSA	-0.00042	-0.00052	-0.00062	-0.00074	-0.00088	-0.00099	-0.00115
XEC	-0.00008	-0.00010	-0.00012	-0.00015	-0.00018	-0.00020	-0.00023
XMN	-0.00045	-0.00055	-0.00066	-0.00079	-0.00094	-0.00106	-0.00122
XSS	-0.00118	-0.00146	-0.00173	-0.00207	-0.00247	-0.00280	-0.00322
XLC	-0.00010	-0.00012	-0.00014	-0.00017	-0.00020	-0.00023	-0.00027
XEU	-0.00000	-0.00000	-0.00000	-0.00000	-0.00000	-0.00000	-0.00000
XHY	-0.00073	-0.00091	-0.00108	-0.00129	-0.00154	-0.00174	-0.00201

Source: Authors.

squared. The denominator in equation (A.16) is a scaling factor such that arrivals are unchanged when δT is equal to zero. The linear parameter takes the value 0.22 and the quadratic parameter is -0.00791. A similar equation defines the departure equation.[7] For departures, α^{dep} is equal to -0.18 and β^{dep} is equal to 0.00483.

$$Arr(\Delta T) = Arr(T^0)\left[\frac{\exp\left(\alpha^{arr}(T^0+\Delta T)+\beta^{arr}(T^0+\Delta T)^2\right)}{\exp\left(\alpha^{arr}(T^0)+\beta^{arr}(T^0)^2\right)}-1\right] \tag{A.16}$$

$$Dep(\Delta T) = Dep(T^0)\left[\frac{\exp\left(\alpha^{dep}(T^0+\Delta T)+\beta^{dep}(T^0+\Delta T)^2\right)}{\exp\left(\alpha^{dep}(T^0)+\beta^{dep}(T^0)^2\right)}-1\right] \tag{A.17}$$

The monetized net impact is provided in equation (A.18), where the relevant costs are provided from the base year data.

$$NetRev^0(\Delta T) = P^{arr}Arr(\Delta T) - P^{dep}Dep(\Delta T) \tag{A.18}$$

The net revenues must sum to zero globally, thus an additive factor is applied to the initial net revenue estimate:

$$NetRev(\Delta T) = NetRev^0(\Delta T) - \chi(\Delta T) \tag{A.19}$$

where

$$\chi(\Delta T) = \sum_r NetRev^0(\Delta T)/N$$

Finally, this is converted to a percent of GDP:

$$Impact^{tou}(\Delta T) = NetRev(\Delta T)/GDP_{2011}$$

Table A.13 reflects the tourism shocks that are input into the bottom-up scenarios. The levels reflect the projected change in tourism revenues derived from the assumed temperature change as a percent of baseline (real) GDP. Rest of East Asia would observe the largest negative impact at nearly 0.6% of GDP in 2050, followed by Rest of Latin America & Caribbean. Many high-income countries are projected to benefit, e.g., Russia, France, the United States, Germany and Canada.

[7] Departures are relative to the home-country temperature, not the destination country.

Table A.13: The projected impact of temperature rise on tourism revenues wrt GDP

	2022	2025	2030	2035	2040	2045	2050
AUS	-0.037	-0.043	-0.045	-0.048	-0.051	-0.052	-0.054
CHN	0.009	0.010	0.010	0.010	0.010	0.010	0.011
JPN	0.004	0.005	0.006	0.007	0.007	0.008	0.009
KOR	0.021	0.024	0.026	0.029	0.033	0.035	0.039
IDN	-0.060	-0.064	-0.061	-0.061	-0.061	-0.060	-0.061
IND	-0.077	-0.083	-0.077	-0.074	-0.075	-0.073	-0.074
CAN	0.132	0.134	0.119	0.112	0.108	0.101	0.098
USA	0.391	0.415	0.367	0.335	0.310	0.278	0.255
MEX	-0.035	-0.041	-0.044	-0.047	-0.050	-0.052	-0.054
ARG	-0.001	-0.001	-0.001	-0.001	-0.001	-0.001	-0.002
BRA	-0.074	-0.084	-0.087	-0.091	-0.095	-0.094	-0.096
FRA	0.238	0.271	0.280	0.298	0.315	0.315	0.319
DEU	0.153	0.177	0.192	0.201	0.205	0.198	0.194
ITA	0.012	0.014	0.015	0.016	0.017	0.017	0.017
GBR	0.041	0.049	0.055	0.062	0.070	0.074	0.080
RUS	0.196	0.227	0.254	0.285	0.318	0.338	0.368
SAU	-0.041	-0.047	-0.051	-0.056	-0.060	-0.062	-0.064
TUR	0.008	0.009	0.009	0.009	0.009	0.009	0.009
ZAF	-0.044	-0.049	-0.047	-0.048	-0.051	-0.053	-0.057
XEA	-0.498	-0.533	-0.518	-0.525	-0.546	-0.550	-0.574
XSA	-0.097	-0.109	-0.107	-0.106	-0.107	-0.105	-0.106
XEC	-0.105	-0.120	-0.126	-0.126	-0.120	-0.109	-0.100
XMN	-0.136	-0.151	-0.148	-0.147	-0.146	-0.138	-0.134
XSS	-0.242	-0.262	-0.239	-0.214	-0.194	-0.168	-0.149
XLC	-0.183	-0.200	-0.200	-0.200	-0.200	-0.192	-0.188
XEU	0.050	0.057	0.061	0.067	0.074	0.079	0.086
XHY	-0.045	-0.052	-0.055	-0.062	-0.071	-0.080	-0.092

Source: Authors.

Appendix B. Concordance with GTAP Data Base

The model is calibrated to version V11_1POW of the GTAP Data Base, which has 162 countries/regions and 76 sectors (64 from the standard GTAP Data Base, plus electricity broken into 12 activities). Table B.14 provides the concordance between GTAP's 162 countries/regions with the 27 modeled regions, which has a focus on the G20.[8] Table B.15 provides the concordance between the 76 sectors of GTAP's Power Data Base to the 30 modeled activities. The aggregation only has 22 commodities as the 9 electricity activities are aggregated to a single commodity.

[8] The G20 is comprised of 19 countries plus the European Union and the African Union (since 2023).

Table B.14: Regional concordance

No.	Region	GTAP Region
1	Australia (AUS)	Australia (AUS)
2	China (CHN)	China (CHN)
3	Japan (JPN)	Japan (JPN)
4	South Korea (KOR)	Republic of Korea (KOR)
5	Indonesia (IDN)	Indonesia (IDN)
6	Rest of East Asia and Pacific (XEA)	Rest of East Asia (XEA), Rest of Oceania (XOC), Mongolia (MNG), Brunei Darussalam (BRN), Cambodia (KHM), Lao People's Democratic Republic (LAO), Malaysia (MYS), Philippines (PHL), Thailand (THA), Viet Nam (VNM), Rest of Southeast Asia (XSE)
7	India (IND)	India (IND)
8	Rest of South Asia (XSA)	Rest of South Asia (XSA), Afghanistan (AFG), Bangladesh (BGD), Nepal (NPL), Pakistan (PAK), Sri Lanka (LKA)
9	Canada (CAN)	Canada (CAN)
10	United States (USA)	United States of America (USA)
11	Mexico (MEX)	Mexico (MEX)
12	Argentina (ARG)	Argentina (ARG)
13	Brazil (BRA)	Brazil (BRA)
14	France (FRA)	France (FRA)
15	Germany (DEU)	Germany (DEU)
16	Italy (ITA)	Italy (ITA)
17	United Kingdom (GBR)	United Kingdom of Great Britain and Northern Ireland (GBR)
18	Russian Federation (RUS)	Russian Federation (RUS)
19	Saudi Arabia (SAU)	Saudi Arabia (SAU)
20	Türkiye (TUR)	Türkiye (TUR)
21	Rest of Europe and Central Asia (XEC)	Albania (ALB), Serbia (SRB), Belarus (BLR), Ukraine (UKR), Kazakhstan (KAZ), Kyrgyzstan (KGZ), Tajikistan (TJK), Uzbekistan (UZB), Rest of Former Soviet Union (XSU), Armenia (ARM), Azerbaijan (AZE), Georgia (GEO)
22	South Africa (ZAF)	South Africa (ZAF)
23	Rest of Middle East and North Africa (XMN)	Bahrain (BHR), Iran (Islamic Republic of) (IRN), Iraq (IRQ), Israel (ISR), Jordan (JOR), Kuwait (KWT), Lebanon (LBN), Oman (OMN), Palestine (PSE), Qatar (QAT), Syrian Arab Republic (SYR), United Arab Emirates (ARE), Rest of Western Asia (XWS), Algeria (DZA), Egypt (EGY), Morocco (MAR), Tunisia (TUN), Rest of North Africa (XNF)
24	Rest of Sub-Saharan Africa (XSS)	Rest of Eastern Africa (XEC), Benin (BEN), Burkina Faso (BFA), Cameroon (CMR), Côte d'Ivoire (CIV), Ghana (GHA), Guinea (GIN), Mali (MLI), Niger (NER), Nigeria (NGA), Senegal (SEN), Togo (TGO), Rest of Western Africa (XWF), Angola (AGO), Central African Republic (CAF), Chad (TCD), Congo (COG), Democratic Republic of the Congo (COD), Equatorial Guinea (GNQ), Gabon (GAB), São Tomé and Príncipe (STP), Burundi (BDI), Comoros (COM), Ethiopia (ETH), Kenya (KEN), Madagascar (MDG), Malawi (MWI), Mauritius (MUS), Mozambique (MOZ), Rwanda (RWA), Sudan (SDN), United Republic of Tanzania (TZA), Uganda (UGA), Zambia (ZMB), Zimbabwe (ZWE), Botswana (BWA), Eswatini (SWZ), Namibia (NAM), Rest of Southern African Customs Union (XSC), Rest of the World (XTW)

Regional concordance, continued

No.	Region	GTAP Region
25	Rest of Latin America and Caribbean (XLC)	Bolivia (Plurinational State of) (BOL), Chile (CHL), Colombia (COL), Ecuador (ECU), Paraguay (PRY), Peru (PER), Uruguay (URY), Venezuela (Bolivarian Republic of) (VEN), Rest of South America (XSM), Costa Rica (CRI), Guatemala (GTM), Honduras (HND), Nicaragua (NIC), Panama (PAN), El Salvador (SLV), Rest of Central America (XCA), Dominican Republic (DOM), Jamaica (JAM), Haiti (HTI), Puerto Rico (PRI), Trinidad and Tobago (TTO), Rest of Caribbean (XCB)
26	Rest of the European Union (XEU)	Austria (AUT), Belgium (BEL), Bulgaria (BGR), Croatia (HRV), Cyprus (CYP), Czechia (CZE), Denmark (DNK), Estonia (EST), Finland (FIN), Greece (GRC), Hungary (HUN), Ireland (IRL), Latvia (LVA), Lithuania (LTU), Luxembourg (LUX), Malta (MLT), Netherlands (NLD), Poland (POL), Portugal (PRT), Romania (ROU), Slovakia (SVK), Slovenia (SVN), Spain (ESP), Sweden (SWE)
27	Rest of high-income countries (XHY)	New Zealand (NZL), China, Hong Kong SAR (HKG), Chinese Taipei (TWN), Singapore (SGP), Rest of North America (XNA), Norway (NOR), Switzerland (CHE), Rest of EFTA (XEF), Rest of Eastern Europe (XEE), Rest of Europe (XER)

Table B.15: Concordance for activities

No.	Activity	GTAP Sector
1	Crops (crp-a)	Paddy rice (PDR), Wheat (WHT), Cereal grains nec (GRO), Vegetables, fruit, nuts (V_F), Oil seeds (OSD), Sugar cane, sugar beet (C_B), Plant-based fibers (PFB), Crops nec (OCR)
2	Livestock and dairy (lvs-a)	Bovine cattle, sheep and goats, horses (CTL), Animal products nec (OAP), Raw milk (RMK), Wool, silk-worm cocoons (WOL)
3	Forestry (frs-a)	Forestry (FRS)
4	Coal extraction (coa-a)	Coal (COA)
5	Oil extraction (oil-a)	Oil (OIL)
6	Gas extraction (gas-a)	Gas (GAS), Gas manufacture, distribution (GDT)
7	Other pimary sectors (oxt-a)	Other Extraction (formerly omn Minerals nec) (OXT)
8	Processed food (pfd-a)	Fishing (FSH), Bovine meat products (CMT), Meat products nec (OMT), Vegetable oils and fats (VOL), Dairy products (MIL), Processed rice (PCR), Sugar (SGR), Food products nec (OFD), Beverages and tobacco products (B_T)
9	Other light manufacturing (xlm-a)	Textiles (TEX), Wearing apparel (WAP), Leather products (LEA), Wood products (LUM)
10	Paper products & publishing (ppp-a)	Paper products, publishing (PPP)

Concordance for activities, continued

No.	Activity	GTAP Sector
11	Chemicals, rubber and plastics (chp-a)	Chemical products (CHM), Basic pharmaceutical products (BPH), Rubber and plastic products (RPP)
12	Non-metallic minerals (nmm-a)	Mineral products nec (NMM)
13	Ferrous metals (i_s-a)	Ferrous metals (I_S)
14	Other metals (nfm-a)	Metals nec (NFM)
15	Other manufacturing (xmn-a)	Metal products (FMP), Computer, electronic and optical products (ELE), Electrical equipment (EEQ), Machinery and equipment nec (OME), Motor vehicles and parts (MVH), Transport equipment nec (OTN), Manufactures nec (OMF)
16	Refined oil (p_c-a)	Petroleum, coal products (P_C)
17	Electricity transmission and distribution (etd-a)	Electricity transmission and distribution (TnD)
18	Solar power (els-a)	Solar power (SolarP)
19	Wind power (elw-a)	Wind power (WindBL)
20	Other renewable power (elr-a)	Other baseload (OtherBL)
21	Hydro power (elh-a)	Hydro power baseload (HydroBL), Hydro power peakload (HydroP)
22	Coal-fired power (elc-a)	Coal power baseload (CoalBL)
23	Gas power (elg-a)	Gas power baseload (GasBL), Gas power peakload (GasP)
24	Oil power (elo-a)	Oil power baseload (OilBL), Oil power peakload (OilP)
25	Nuclear power (eln-a)	Nuclear power (NuclearBL)
26	Construction (cns-a)	Construction (CNS)
27	Air transport (atp-a)	Air transport (ATP)
28	Water transport (wtp-a)	Water transport (WTP)
29	Other transport (otp-a)	Transport nec (OTP)
30	Services (srv-a)	Water (WTR), Trade (TRD), Accommodation, Food and service activities (AFS), Warehousing and support activities (WHS), Communication (CMN), Financial services nec (OFI), Insurance (formerly isr) (INS), Real estate activities (RSA), Business services nec (OBS), Recreational and other services (ROS), Public Administration and defense (OSG), Education (EDU), Human health and social work activities (HHT), Dwellings (DWE)

Note. The commodity concordance is largely the same with the exception that the 9 electricity activities are aggregated into a single commodity, for a total of 22 commodities.

Appendix C. Additional figures and tables

Table C.16: Amplification (%) through international spillovers

	2030	2040	2050
Top-down: K+L	1.1	3.0	5.5
Top-down: K+L+T+R	2.0	3.3	3.8
Bottom-up: SLR+AGR+LAB+HLT	6.0	4.9	4.0

Note: Calculated as the percentage increase of welfare costs in the global scenario compared to the sum of domestic impacts for region-by-region scenarios.

Table C.17: Welfare impacts (%)

	Top-Down: K+L				Bottom-up: SLR+AGR+LAB+HLT			
	Domestic	Total	Share of domestic in total	Share of foreign in total	Domestic	Total	Share of domestic in total	Share of foreign in total
RUS	1.07	1.05	102.27	-2.27	0.01	-0.04	-21.53	121.53
CAN	0.89	0.79	113.04	-13.04	0.02	0.17	12.40	87.60
DEU	0.39	0.42	94.13	5.87	0.00	-0.03	-4.14	104.14
GBR	0.25	0.26	99.58	0.42	0.00	-0.04	-5.83	105.83
XEU	0.26	0.24	106.40	-6.40	0.00	-0.01	12.89	87.11
XEC	0.16	0.11	149.67	-49.67	0.01	0.08	7.43	92.57
FRA	0.19	0.18	102.59	-2.59	0.00	0.00	1.23	98.77
KOR	0.09	0.08	105.07	-5.07	-0.03	-0.05	53.14	46.86
XHY	0.01	-0.05	-15.22	115.22	-0.55	-0.59	92.93	7.07
ITA	-0.07	-0.07	101.77	-1.77	0.00	0.01	-80.56	180.56
USA	-0.12	-0.13	92.82	7.18	-0.10	-0.10	97.27	2.73
JPN	-0.20	-0.20	100.23	-0.23	-0.03	-0.04	70.39	29.61
CHN	-0.23	-0.23	99.18	0.82	-0.42	-0.46	91.11	8.89
TUR	-0.23	-0.28	82.49	17.51	-0.15	-0.05	312.14	-212.14
AUS	-0.31	-0.40	79.15	20.85	-0.21	-0.19	112.95	-12.95
ARG	-0.33	-0.42	78.65	21.35	-0.12	0.03	-357.31	457.31
MEX	-0.55	-0.59	93.90	6.10	-0.14	-0.12	118.80	-18.80
XLC	-0.70	-0.75	92.78	7.22	-0.14	-0.10	146.67	-46.67
ZAF	-0.72	-0.80	90.33	9.67	-0.44	-0.48	92.74	7.26
BRA	-1.02	-1.08	94.10	5.90	-0.57	-0.50	113.59	-13.59
XMN	-1.09	-1.15	94.66	5.34	-1.17	-1.31	88.96	11.04
IDN	-1.02	-1.07	94.97	5.03	-0.66	-0.62	105.73	-5.73
XEA	-1.12	-1.23	91.03	8.97	-1.30	-1.24	104.69	-4.69
XSA	-0.98	-0.98	99.54	0.46	-1.26	-1.38	91.54	8.46
XSS	-1.04	-1.09	94.66	5.34	-1.64	-1.70	96.86	3.14
IND	-0.81	-0.81	100.08	-0.08	-2.54	-2.64	96.29	3.71
SAU	-1.92	-2.00	96.11	3.89	-2.77	-3.14	88.16	11.84